SUBBAND FILTERING OF FNIRS DATA FROM SCHIZOPHRENIC SUBJECTS

by

ERCAN KARA

B.Sc., in Electronics Engineering, F.M.V. IŞIK University, 2004

Submitted to the Institute of Biomedical Engineering
in partial fulfillment of the requirements
for the degree of
Master of Science
in
Biomedical Engineering

Boğaziçi University
January 2008

SUBBAND FILTERING OF FNIRS DATA FROM SCHIZOPHRENIC SUBJECTS

APPROVED BY:

Asst. Prof. Ata Akın .....
(Thesis Advisor)

Assoc. Prof. Yasemin Kahya .....

Prof. Dr. Yankı Yazgan .....

DATE OF APPROVAL: 22.01.2008

ACKNOWLEDGMENTS

I would like to express my gratitude to all those who gave me the possibility to complete this thesis.

First, I would like to thank my thesis advisor, Asst. Prof. Ata Akın, for his guidance, encouragement and support.

I am deeply indebted to Barış Özkerim, Nermin Topaloğlu, Sinem Serap and Esin Karahan for their friendship and help.

Also, I am extremely grateful to my friends in the Biophotonics Laboratory for their enduring support throughout my thesis. In particular I would like to express my gratitude to Ömer Şaylı, Deniz Duru, Koray Çiftçi and Uzay Emir.

Last, I would like to thank my family for their moral support and patient.

ABSTRACT

SUBBAND FILTERING OF FNIRS DATA FROM SCHIZOPHRENIC SUBJECTS

Schizophrenia is a neurological disorder and typically persists for a life. Investigation of the cerebral hemodynamics of schizophrenic patients with a rapid, non-invasive and precise technique is required to improve the prognosis and guide therapeutic interventions.

Functional Near-Infrared Spectroscopy (fNIRS) is a non-invasive brain imaging technique measuring the changes in oxy-hemoglobin and deoxy-hemoglobin particularly in prefrontal cortex.

In this study, fNIRS was used during a Stroop task to investigate the differences in oscillatory dynamics between schizophrenic patients and control subjects. Spectral analysis and dyadic wavelet transform were employed to quantify the degree of loss of cerebral activation and to localize the major areas of loss of activation in the prefrontal cortex.

In this study, it was found that specific brain areas are responsible for generating specific oscillatory patterns and energies of these patterns are significantly reduced in schizophrenic patients.

Keywords: Schizophrenia, Functional Near Infrared Spectroscopy (fNIRS), Spectral Analysis, Wavelet Decomposition, Stroop Task.

ÖZET

ŞİZOFREN DENEKLERDEN ALINAN İŞLEVSEL YAKIN KIZILÖTESİ SPEKTROSKOPİ VERİLERİNİN ALTBAND FİLTRELENMESİ

Şizofreni sinirbilimsel bir bozukluktur ve genelde hayat boyunca devam eder. Şizofreni hastalarının beyinsel hemodinamiklerinin hızlı, noninvazif ve keskin sonuçlar veren bir teknikle incelenmesi, hastalığın tahmini ve tedavi edici müdahalelerde bulunma açısından gereklidir.

İşlevsel yakın kızıl ötesi spektroskopi, özellikle prefrontal korteksteki oksijenli hemoglobin ve oksijensiz hemoglobin miktarındaki değişimleri ölçmek için kullanılan noninvazif beyin görüntüleme tekniğidir.

Bu çalışmada, şizofren ve sağlıklı deneklerin, salınımsal dinamik farklarını incelemek için işlevsel yakın kızıl ötesi spektroskopi ve Stroop test kullanılmıştır. Beyinsel aktivasyon kayıplarının derecesini ve bu kayıpların prefrontal korteksteki başlıca bölgelerin yerini belirlemek için spektral çözümleme ve dalgacık ayrışması teknikleri kullanılmıştır.

Bu çalışmada, beyindeki belli bölgelerin özgül salınımsal paternler ürettiği ve bu paternlerin enerjisinin şizofren hastalarda daha düşük olduğu bulunmuştur.

Anahtar Sözcükler: Şizofreni, İşlevsel Yakın Kızıl Ötesi Spektroskopi, Spektral Çözümleme, Dalgacık Ayrışması, Stroop Test.

TABLE OF CONTENTS

LIST OF FIGURES

LIST OF TABLES

LIST OF SYMBOLS

$deoxy - Hb$	Deoxy-hemoglobin
$oxy - Hb$	Oxy-hemoglobin
Hb	Deoxy-hemoglobin Concentration
HbO_2	Oxy-hemoglobin Concentration
ε_{Hb}	Absorption Coefficient of Deoxy-hemoglobin
ε_{HbO_2}	Absorption Coefficient of Oxy-hemoglobin
I	Transmitted Light Intensity
I_0	Incident Light Intensity
L	Optical Pathlength
OD	Optical Density
λ_1	Wavelength 1
λ_2	Wavelength 2

LIST OF ABBREVIATIONS

ANOVA	Analysis of Variance
BA	Brodmann Area
CBF	Cerebral Blood Flow
CBV	Cerebral Blood Volume
CPT	Continuous Performance Test
EEG	Electroencephalogram
ERPs	Event-Related Brain Potentials
fMRI	Functional Magnetic Resonance Imaging
HB	Deoxy-Hemoglobin
HBO2	Oxy-Hemoglobin
HF	High Frequency
LF	Low Frequency
LN	Letter Number
MDT	Mirror Drawing Task
MEG	Magnetoencephalography
NIRS	Near Infrared Spectroscopy
PET	Positron Emission Tomography
PFC	Prefrontal Cortex
RC	Ruler-Catching
RNG	Random Number Generation
SFT	Sequential Finger-To-Thumb
SPECT	Single-Positron Emission
VFT	Verbal Fluency
VLF	Very Low Frequency

1. INTRODUCTION

Schizophrenia is characterized by a loss of contact with reality and a disruption of thought, perception, mood, and movement. The disorder typically becomes apparent during adolescence or early adulthood and usually persists for life. The name, introduced in 1911 by Swiss psychiatrist Eugen Bleuler, roughly means "divided mind", because of his observation that many patients seemed to oscillate between normal and anormal states. There are, however, many variations in the manifestations of schizophrenia, including those that show a steadily deteriorating course. Indeed, it is still not clear whether what is called schizophrenia is a single disease or several [1].

Computerized tomography, magnetic resonance imaging, and cerebral blood flow studies have revealed that some patients with schizophrenia have one or more of four major anatomical abnormalities. First, early in the disease there is a reduction in the blood flow to the left globus pallidus, suggestive of a disturbance in the system that connects the basal ganglia to the frontal lobes. Second, there appears to be a disturbance in the frontal lobes themselves since blood flow does not increase during tests of frontal function involving working memory, as it does in normal subjects. Third, the cortex of the medial temporal lobe is thinner and the anterior portion of the hippocampus is smaller than in normal people, especially on the left side, consistent with a defect in memory. Finally, the lateral and third ventricles are enlarged and there is widening of the sulci, especially in the thinner temporal lobe and in the frontal lobe, reflecting a reduction in the volume of this lobe as well [2].

To date, several functional neuroimaging techniques have been tested on schizophrenics while they were performing several cognitive psychophysics tasks. The challenge in all these studies has been to converge to a rapid, non-invasive and precise technique.

We have decided to apply the functional near infrared spectroscopy (fNIRS) measurement during cognitive activity to reproduce the similar differences observed by

other modalities. Since optical imaging techniques offer rapid and non-invasive access to brain oxygenation and blood flow, we decided to investigate the cerebral the cerebral activation during a color-word matching Stroop task.

The problems we addressed are listed below

1. Is it possible to quantify the degree of loss of cerebral activation in schizophrenics by NIRS?
2. Is it possible to localize the major areas of loss of activation?
3. Are there any further dynamics within these activities that might elucidate the loss of activation and hence help us understood the pathophysiology in a more precise manner?

1.1 Motivation and Objective

Early detection of schizophrenia and understanding its pathophysiology might improve prognosis and guide therapeutic interventions. Hence, a rapid, non-invasive and precise means of investigation of the cerebral dynamics of these patients is required. We have decided to use the fNIRS imaging modality during a Stroop task and investigate the oscillatory dynamics between controls and patients. The techniques we employed were the band pass filtering and dyadic wavelet transform.

Our results show that there are specific brain areas responsible for generating specific oscillatory patterns and that these are significantly reduced in schizophrenics.

2. PRINCIPLES OF FUNCTIONAL NEAR INFRARED SPECTROSCOPY

Neuroimaging is a technique used for obtaining structural and functional images of the nervous system, i.e., the peripheral nervous system, the spinal cord and the brain.

Brain activity is associated with a number of physiological events. By using optical techniques, two of these events can be assessed. During neural activity, ionic fluxes across the cell's membrane (e.g., shifts in sodium and potassium ions) result in a change in the membrane potential. The ionic fluxes also cause changes in the magnetic and electrical fields, which, when summed across a large number of synchronously activated neurons, can be assessed using EEG or MEG. Neuronal activity is fueled by glucose metabolism, so increases in neural activity result in increased glucose and oxygen consumption from the local capillary bed. A reduction in local glucose and oxygen stimulates the brain to increase local arteriolar vasodilation, which increases local cerebral blood flow (CBF) and cerebral blood volume (CBV), a mechanism known as neurovascular coupling. Over a period of several seconds, the increased CBF carries both glucose and oxygen to the area, the latter of which is transported via oxygenated hemoglobin in the blood. The increased oxygen transported to the area typically exceeds the local neuronal rate of oxygen utilization, resulting in an overabundance of cerebral blood oxygenation in active areas [3]. Although the initial increase in neural activity is thought to result in a focal increase in deoxygenated hemoglobin in the capillary bed as oxygen is withdrawn from the hemoglobin for use in the metabolization of glucose, this feature of the vascular response has been much more difficult to measure, and more controversial, than hyperoxygenation [4].

Because oxygenated and deoxygenated hemoglobin (oxy-Hb, deoxy-Hb) have characteristic optical properties in the visible and near-infrared light range, the change in concentration of these molecules during neurovascular coupling can be measured using optical methods [5]. The most commonly used method of near-infrared spec-

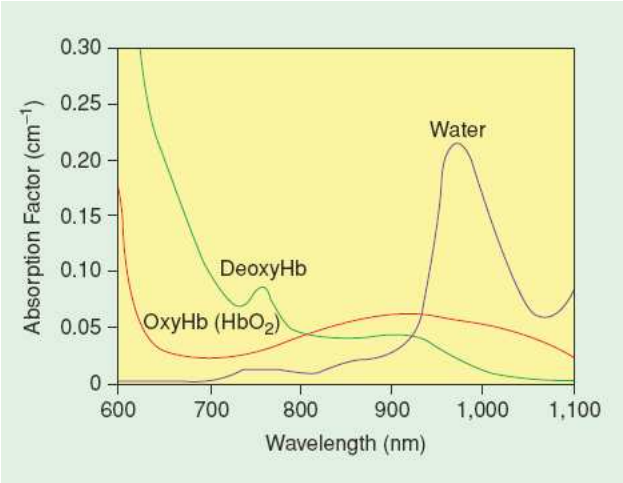

Figure 2.1 The absorption spectrum of chromophores [4].

troscopy measures changes in the ratio of oxy-Hb to blood volume. Most biological tissues are relatively transparent to light in the near-infrared range between 700 - 900 nm, largely because water, a major component of most tissues, absorbs very little energy at these wavelengths (Fig. 2.1).

However, the chromophores oxy-Hb and deoxy-Hb do absorb a fair amount of energy in this range. As such, this spectral band is often referred to as the optical window for the noninvasive assessment of brain activation. In optical window, light penetrates the biological tissue such as the skull quite easily and can thus be injected into the head. In cerebrum, near infrared light is mainly absorbed by oxy-Hb and deoxy-Hb. The fraction of light that is not absorbed on its path within the cerebrum can in part be detected by an optical probe when it leaves the head again. If near infrared light is emitted from the scalp surface and the reflected light is detected in a distance of 2-5 cm from the light source at the scalp surface again, the injected light travels in a "banana shape" form from source to detector passing through the subjacent brain tissue, as illustrated in Figure 2.2. From the amount of reflected(i.e, not absorbed) near infrared light, it is now possible to calculate changes in the concentration of oxy-Hb and deoxy-Hb in living brain tissue using a modified Beer-Lambert law (Appendix A), employing near infrared light absorption characteristics and two wavelength absorption data. By adding the concentration changes of oxy-Hb and deoxy-Hb, the third vascular

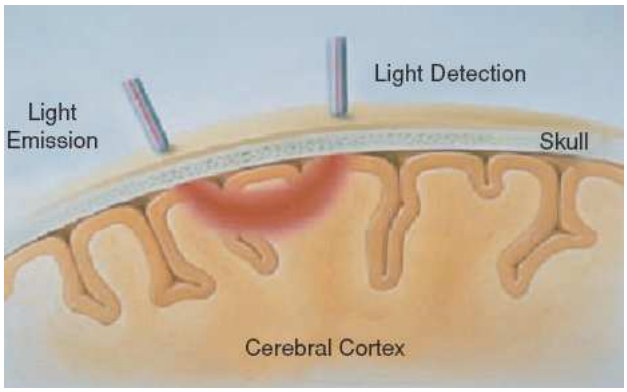

Figure 2.2 Banana-shaped photon path [4].

parameter can be obtained (total hemoglobin, total-Hb), which corresponds to the corpuscular blood volume [6, 4].

For the consideration of penetration depth of near infrared light, photon migration models predicted it to be directly proportional to the inter optode distance. There is an agreement on the fact that when used on the scalp surface, NIRS can detect the changes in hemoglobin concentration on the cortical surface, although the signal may be limited to the top 2-3 mm of the cortex.

The underlying idea is that when brain activity increases within the a particular part of the cerebral cortex, blood supply to that area increases as well, as does the level of oxy-Hb. The consumption of oxygen during brain activity furthermore leads to an increase in deoxygenated hemoglobin that is, however, soon compensated by the increase in blood supply, and deoxy-Hb usually decreases as a result. In other words, activation of a particular brain region is supposed to be reflected in an increase in oxy-Hb and total-Hb and a corresponding decrease in deoxy-Hb. These changes in the concentration of oxy-Hb and deoxy-Hb can now be detected by means of NIRS [6].

3. FUNCTIONAL NEUROIMAGING IN SCHIZOPHRENIA

Advances in neuroimaging technologies have greatly facilitated our understanding of brain function in psychiatric and neurological disorders such as schizophrenia, mood disorders, anxiety disorders, Alzheimer's disease, Parkinson's disease, epilepsy, traumatic brain injury, and personal disorders. Neuroimaging techniques such as electroencephalography (EEG), event-related brain potentials (ERPs), magnetoencephalography (MEG), positron emission tomography (PET), single-positron emission computed tomography (SPECT), and functional magnetic resonance imaging (fMRI) have permitted significant advances in our understanding of the neurobiological substrates of many of these brain disorders. In addition, each of the neurophysiological/neuroimaging techniques used the study these brain processes has its own inherent limitations. In comparison to traditional neuroimaging technologies, emerging techniques such as functional near infrared spectroscopy (fNIRS) offer relatively non-invasive, safe, portable, low-cost methods of monitoring of brain activity [7].

In addition to functional imaging studies, recent research revealed abnormalities of various neurotransmitter systems in the prefrontal regions, such as Brodmann areas 9, 10 and 46 (Figure 3.1). Affected neurotransmitters include acetylcholine, serotonin, glutamate, γ-aminobutyric acid and choleccystokinin. Disorder of synaptic formation, cytoarchitecture, and glial components were also suggested in the same regions. These biochemical and morphologic changes support the role of prefrontal cortex in the pathophysiology of schizophrenia [8].

Neuroimaging studies have identified schizophrenia as being associated with dysfunction of the prefrontal cortex. The prefrontal parts play an important role in schizophrenia. The dorsolateral prefrontal cortex is the most commonly affected prefrontal site (BA 46). Until recent studies, most of the studies show that the physiologic abnormality in this brain region was seen as hypofrontality. However, hyperfrontality in schizophrenic patients was observed in some researches. Manoach concluded that

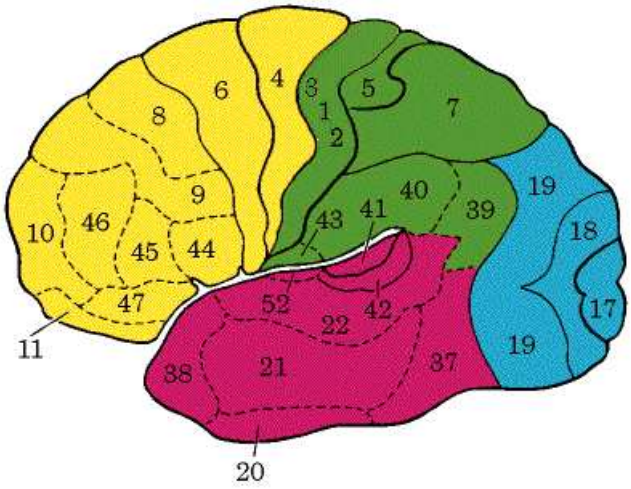

Figure 3.1 Broadmann Areas - Sagital View.

both hypofrontality and hyperfrontality should be considered as valid and informative reflections of prefrontal cortex dysfunction in schizophrenia [9]. Quantana et al. said that the manifestation of the prefrontal dysfunction depends on task specifications and effects of the task in corresponding areas [10, 11].

3.1 Functional Near Infrared Spectroscopy In Schizophrenia

Okada et al. utilized multi-channel fNIRS to investigate disturbances in interhemispheric integration of brain oxygen metabolism and hemodynamics. They utilized a mirror drawing task (MDT) and found that controls showed distinct and well-integrated patterns of changes in oxy-Hb, deoxy-Hb, and total blood volume during the MDT. In contrast, half of the patients with schizophrenia showed "dysregulated patterns" in the frontal regions between hemispheres, such that increases in oxy-Hb were not paralleled by decreases in deoxy-Hb. This led the authors to suggest that certain symptoms of schizophrenia might be related to problems in interhemispheric integration [7, 12].

Similarly, Fallgatter and Strik examined the relationship between lateralized frontal fNIRS activation patterns during the execution of a continuous performance test

(CPT). Interestingly, they did not find any overall or hemispheric activation effects in their cohort. However, when compared to healty controls they found group differences, with a lateralized activation in schizophrenia. Furthermore, a trend towards higher left relative to right oxy-Hb and deoxy-Hb ratios at rest and during activation were observed in subjects with schizophrenia. This led the authors to suggest that there may be a reduced specific lateralized frontal activity, possibly based on a left hemisphere functional deficit in schizophrenia [7, 13].

Another more recent investigation has utilized frontally based tasks such as random number generation (RNG), ruler-catching (RC), and sequential finger-to-thumb (SFT) tasks to show that there are task dependent functional abnormalities frontal brain metabolism in schizophrenia [8]. Specifically, during the RNG task, total-Hb and oxy-Hb concentrations increased and deoxy-Hb decreased, but the responses were significantly smaller in schizophrenic patients. During RC task, oxy-Hb in patients with schizophrenia tended to decrease, in contrast to the mostly increasing response in control subjects. No group difference was observed during the SFT task [7, 8].

Verbal fluency tests (VFTs) have also been utilized to clarify the nature of language-related problems in schizophrenia. Kubota et al. found that while healthy subjects performed both semantic and phonemic fluency equivalently, subjects with schizophrenia showed more compromised performance in semantic VFTs compared to the phonemic VFTs. FNIRS measurement revealed that the pattern of prefrontal cortex (PFC) activation was greater during the phonemic VFT when compared to the semantic VFT in healthy subjects, suggesting more prominent PFC involvement in phonemic-cued retrieval. In contrast, subjects with schizophrenia showed the opposite pattern of activation, implying that the semantic mode of lexical access might impose greater cognitive demands on the PFC for this patient group [7, 14].

Similarly, another study also utilized VFT to demonstrate characteristic time courses of oxy-Hb changes in the frontal lobe for schizophrenia as compared to a sample depressed patients [15]. Specifically, depressed patients demonstrated smaller oxy-Hb increases during the first half of the task period, while patients with schizophrenia had

a small trough of oxy-Hb at the start of the task period and oxy-Hb reincrease in the post-task period. The decreased oxy-Hb activation in depression was consistent with decreased regional cerebral blood flow and metabolism in the dorsolateral prefrontal cortex in the resting state observed in functional neuroimaging studies using other methodologies such as PET, SPECT, and fMRI. Yet these results did not support either the hypofrontolity [16] observed when the task performances of schizophrenic patients are poorer, or the hyperfrontality [17] observed when the task performaces matched. This might be related to the authors' modification to their VFT task (increased length) due to their interest in monitoring time cource changes in blood volume [7].

In contrast, Watanabe and Kato showed findings consistent with task dependent functional hypofrontality demonstrated by other neuroimaging studies [18]. They found that oxy-Hb increased during VFT and letter-number (LN) sequencing, schizophrenia patients showed lower performance and a smaller increase in oxy-Hb during VFTs than controls. This reduced oxy-Hb response during VFTs in schizophrenia patients was also observed even when their performance was matched with controls' performance. In contrast, increase in oxy-Hb during LN in schizophrenia patients was comparable with that of controls. In addition, patients medicated with atypical antipsychotics showed a larger increase in oxy-Hb during VFT and LN than those medicated with typical antipsychotics [7, 18].

Perlstein et al. applied n-back sequential-letter working memory task to schizophrenic patients and control subjects. According to fMRI results, schizophrenic patients showed a deficit in physiological activation of the right dorsolateral prefrontal cortex (BA 46/9) in the context of normal task-dependent activity in other regions, but only under the condition that distinguished them from comparison subjects on task performance. Patients with greater dorsolateral prefrontal cortex dysfunction performed more poorly. Dorsolateral prefrontal cortex dysfunction was selectively associated with disorganization symptoms.

4. STROOP PERFORMANCE IN SCHIZOPHRENIA

Stroop task is a classical neuropsychological test of frontal lobe function often employed in both clinical and research settings. As its basic principle, it comprises of a conflict between certain stimulus dimensions, typically between a color word name and its ink color, thus creating interference between word reading and color naming. The areas specifically activated by the Stroop interference condition have been extensively studied by means of both fMRI and PET. Besides the anterior cingulate cortex, functional neuroimaging studies have repeatedly found several areas of the frontal cortex that seem to be specifically activated during Stroop interference, particularly within left inferior-frontal (BA 44,45 and 47) and frontopolar (BA 10) regions as well as in the inferior part of the left precentral gyrus(BA 6) [6].

In Stroop task, subjects are asked to name the color of ink in which color words printed. There are three conditions: neutral (a noncolor word printed in some ink color, such as XXXX written in blue ink), congruent (color and word are the same, such as Turkish word of BLUE written in a blue ink), incongruent (color and word conflict, such as Turkish word of GREEN written in blue ink) as illustrated in Figure 4.1.

Barch and Carter show that schizophrenic patients exhibits an increased reaction time for each type of stimulus as compared with healthy controls. Interesting point is that mean reaction times of schizophrenic patients and control subjects for neutral stimulus is longer than that for congruent stimulus. The same situation is valid for the mean error rates. In other words, both group's error rate is higher in congruent stimulus.

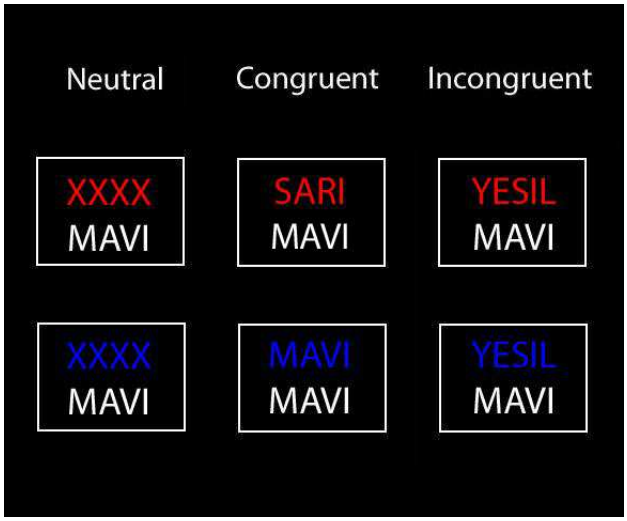

Figure 4.1 Examples of single trials for the neutral, congruent and incongruent condition of the Stroop task. For the upper three examples, the correct answer would be "no", for the lower three examples, the correct answer would be "yes" [27].

5. METHOD

5.1 Subjects

Twelve healthy control participants and twenty seven schizophrenic patients (age, 34.69 $\pm$ 10.31 years) were involved in this study. Healthy control subjects had no history of psychiatric or neurologic disorders. Data from healthy control participants were acquired at Biomedical Engineering Laboratories in Boğaziçi University. Data from schizophrenic patients were acquired at Department of Psychiatry of Pamukkale University Medical Faculty in Denizli, Turkey. Written inform consent was obtained from each subject for participation in this study. The protocol has been approved by the Ethics Board of both Pamukkale and Boğaziçi Universities.

5.2 Experimental Procedure

Each participant sat on a chair with their eyes open during experiments as shown in Figure 5.1. The participants were instructed to minimize movement such as head movements during the NIRS measurements because they might produce artifacts or changes in cerebral perfusion unrelated to the task. Furthermore, experiments were performed in a silent and dimmed room to prevent any other nuisance.

In this study, the color-word matching Stroop task was used to explore the differences in frontal lobe functions between schizophrenia and control subjects. Two rows of letters appeared on the screen and subjects were instructed to decide, whether the color of the top row letters corresponds to the color name written on the bottom row. If the answer is yes, they were instructed to press the right button of the mouse. If the answer is no, they were instructed to press the left button of the mouse. Participants used only their right hands.

Figure 5.1 Experimental Setup [21].

During the neutral trials, the letters in the top row were "XXXX" printed in red, green, blue or yellow, and the bottom row consisted of Turkish color words of "RED", "GREEN", "BLUE", and "YELLOW" printed in white. For congruent trials, the top row consisted of the Turkish color words of "RED", "GREEN", "BLUE", and "YELLOW" printed in the congruent color. For the incongruent condition, the color word was printed in a different color to produce interference between color word and word name.

At the beginning of the experiment, fixation point ("+" sign) was displayed for one minute on the screen. An experiment consisted of 15 block stimuli (5 neutral, 5 congruent and 5 incongruent) in a random order. Each block consisted of 6 trials. Between each blocks, there was a 20 sec wait and fixation point was displayed on the screen. Word remained on the computer screen until the response was given with a maximum time of 4 sec. The screen was blank between the trials.

Subjects were tested prior to the experiment with a small version of Stroop task for training.

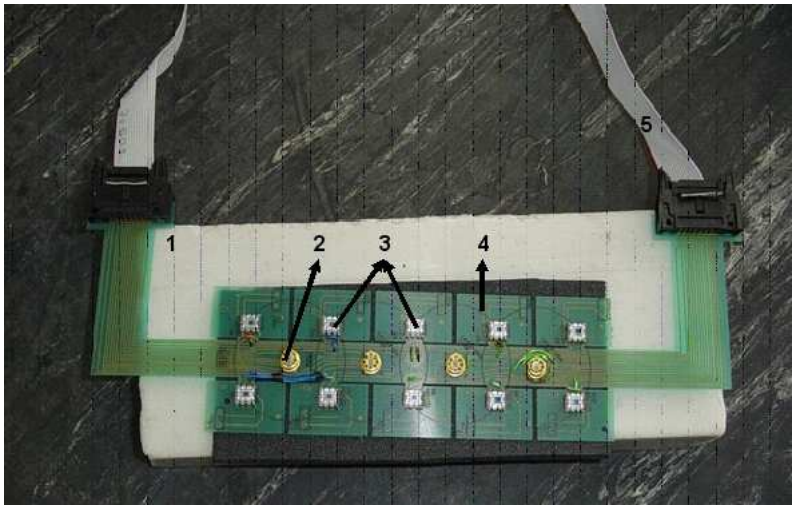

Figure 5.2 16 channels Niroxcope Probe 1-Grey Phantom 2- LED 3- Detectors 4- PCB 5- Cable [21].

5.3 Data Acquisition By NIRS

Hemodynamic changes in the prefrontal cortex were measured using NIROXCOPE 301 which was developed at the Biophotonics Laboratory of the Institute of Biomedical Engineering in Boğaziçi University. NIROXCOPE 301 is composed of

Flexible Sensor that consists of four LED light sources and ten detectors which covers forehead as shown in Figure 5.2. The distance between source and detector is 2.5 cm. The LED light sources can emit at three wavelenghts of 730nm, 805nm and 850nm. The detectors are sensitive in the near infrared spectrum.

Control Box mainly consists of transmitter, receiver circuits and usb data acquisition card

Software that controls the device and store the data on the computer for offline analysis

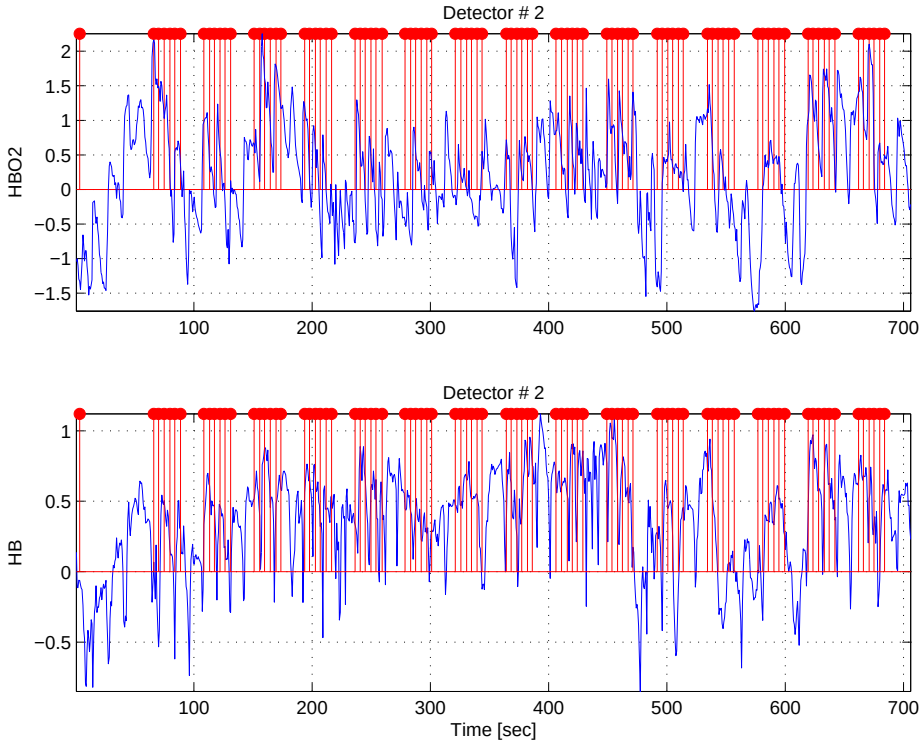

Figure 5.3 Oxy-Hb and deoxy-Hb changes during the Stroop task from schizoprenic patient.

5.4 Analysis of fNIRS Data and Statistics

Signal changes at the detectors during the Stroop task was collected by means of NIROXCOPE 301. Oxy-Hb and deoxy-Hb changes were calculated by using the modified Beer Lambert law (Appendix A). Figure 5.3 and 5.4 show the oxy-Hb and deoxy-Hb changes of schizophrenic patient and control subject during the Stroop task respectively. The red lines show the time stimulus was applied.

In the first part of our study, analysis of hemodynamic signals in the frequency domain was performed. The algorithm of frequency domain analysis is shown in Figure 5.5. After the calculation of oxy-Hb and deoxy-Hb signals, the butterworth low pass filter with a cut off frequency of 0.25 Hz was used to eliminate the fluctuations due to heart rate, respiration etc. Fourth order band pass butterworth filter was used to separate the oxy-Hb and deoxy-Hb signals into very low frequency (VLF) (0.02 - 0.05 Hz), low frequency (LF) (0.08 - 0.12 Hz) and high frequency (HF) (0.12 - 0.18 Hz)

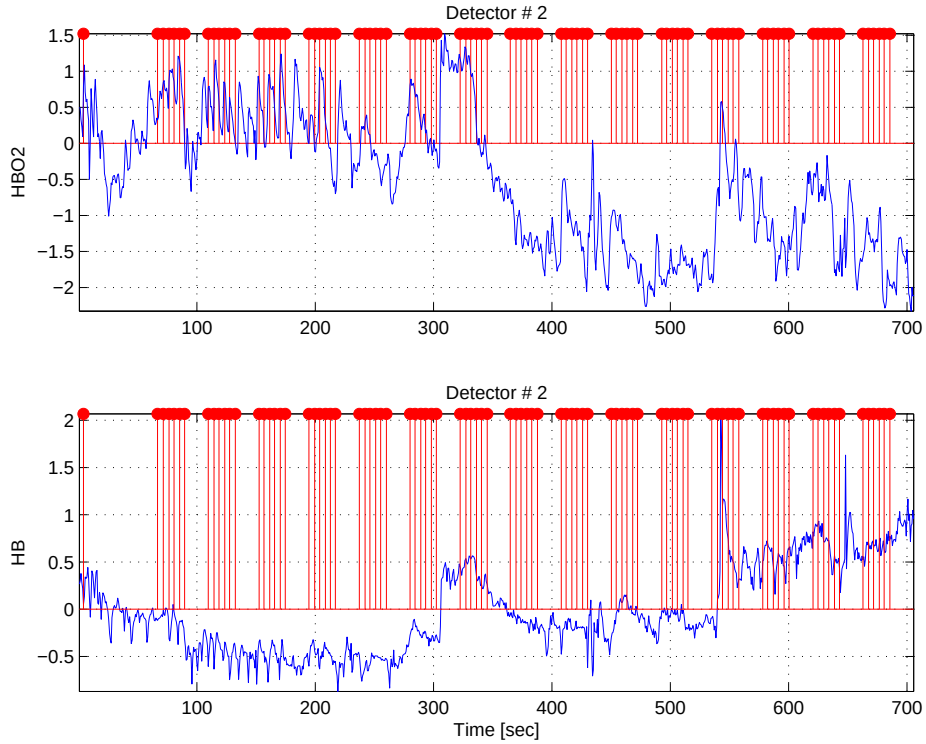

Figure 5.4 Oxy-Hb and deoxy-Hb changes during the Stroop task from control participant.

bands. These bands were found partly from the literature and partly as a result of retrospective spectral analysis. The VLF band has been shown to carry information regarding the main frequency lobe of the hemodynamic response by several authors. While the LF band is known to represent the vasomotor reactivity and is named the Mayer's wave. In a previous study, (not published) we have seen the emergence of a third band that is speculated to reflect the control of autonomic nervous system on vasomotor dynamics. Hence, the choice of the band intervals were mainly arbitrary. The energies of the signals for the neutral, congruent and incongruent trials were computed in each frequency band for each detector. Figure 5.6 shows the means of deoxy-Hb signal with a standard deviation during incongruent trials for each detector in very low, low and high frequency bands. As seen from the figure, it is difficult to differentiate the energies of schizophrenic patients and healthy controls. Therefore, ANOVA test was used to compare the energies of deoxy-Hb and oxy-Hb signals of the schizophrenic patients and control subjects in the very low, low and high frequency bands. The statistically significant level is $p<0.05$. The results of ANOVA will be

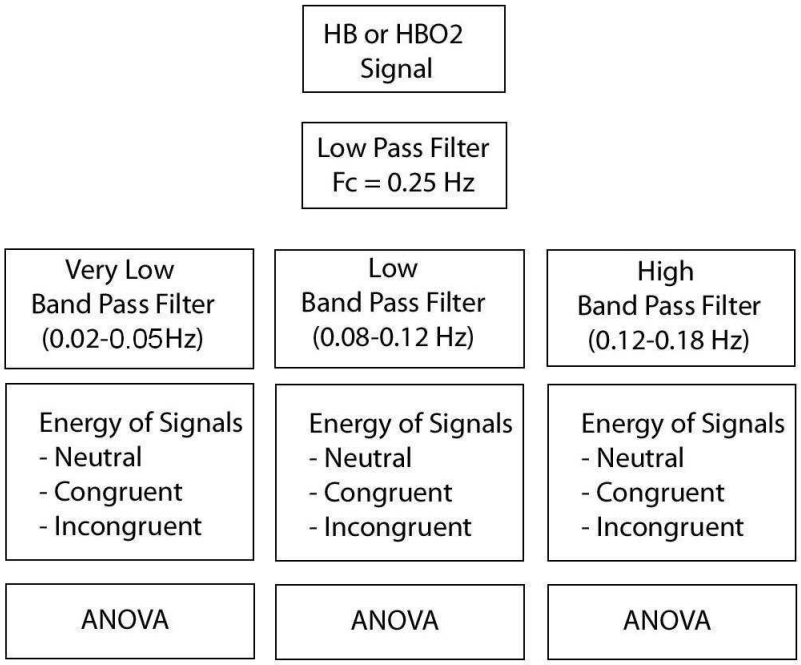

Figure 5.5 Algorithm of frequency domain analysis.

discussed in Results and Discussion section.

In the second part of the thesis, wavelet decomposition analysis was performed. Wavelet transform offers unguided division of the spectral band resulting in a more precise approach to the choice of significantly different frequency bands between two groups. The signal processing algorithm is shown in Figure 5.7. Oxy-Hb and deoxy-Hb signals were decomposed using a five level wavelet decomposition. Daubechies 10 ('db10') was used for decomposition. The frequency bands are:

- A5→ [0, Fs/64] Hz ≅ [0, 0.026] Hz
- D5→ [Fs/64, Fs/32] Hz ≅ [0.026, 0.053] Hz
- D4→ [Fs/32, Fs/16] Hz ≅ [0.053, 0.11] Hz
- D3→ [Fs/16, Fs/8] Hz ≅ [0.11, 0.21] Hz
- D2→ [Fs/8, Fs/4] Hz ≅ [0.21, 0.42] Hz
- D1→ [Fs/4, Fs/2] Hz ≅ [0.42, 0.85] Hz

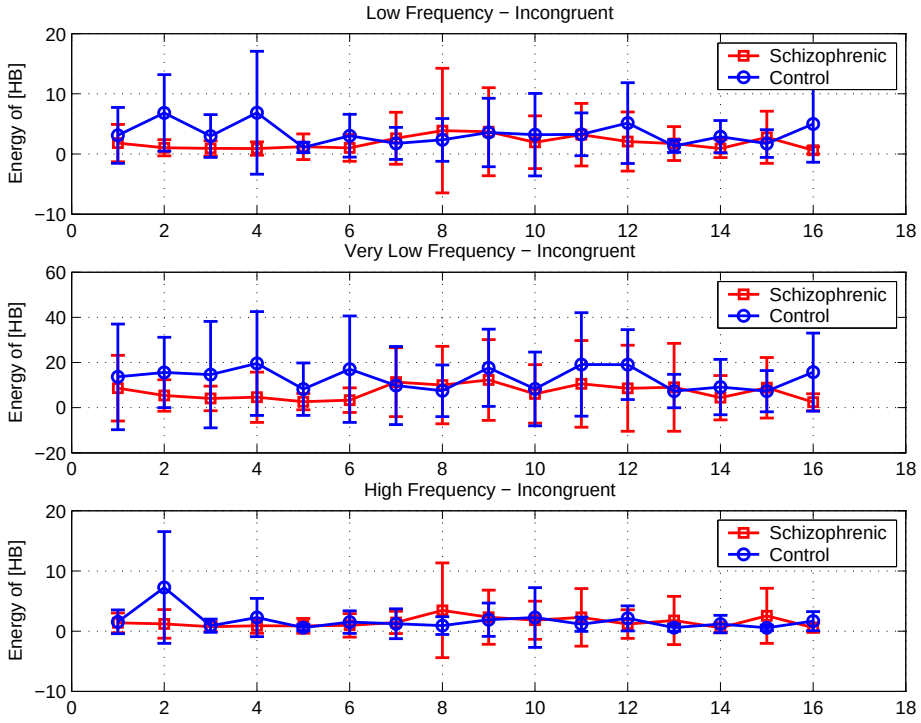

Figure 5.6 HB signal for the incongruent trials.

D5 band (0.026-0.053 Hz) roughly corresponds to very low frequency band in spectral analysis method. Also, D4 (0.053-0.11 Hz) and D3(0.11-0.21 Hz) bands correspond to low frequency and high frequency bands respectively.

Figure 5.8 shows the original and decomposed oxy-Hb signals as an example. After the decomposition, the energy of each subband signal for each detector was calculated. Then, the energy of the oxy-Hb and deoxy-Hb during the neutral, congruent and incongruent trials was computed.

In order to compare data from schizophrenic patients and healthy control group, one-way ANOVA was used. The statistically significant level of difference is taken as $p<0.05$. It indicates that one group mean is significantly different from the other. The results of ANOVA will be discussed in Results and Discussion section.

Also, we employed brain mapping technique whose software was developed at the Institute of Biomedical Engineering in Boğaziçi University to localize the activities

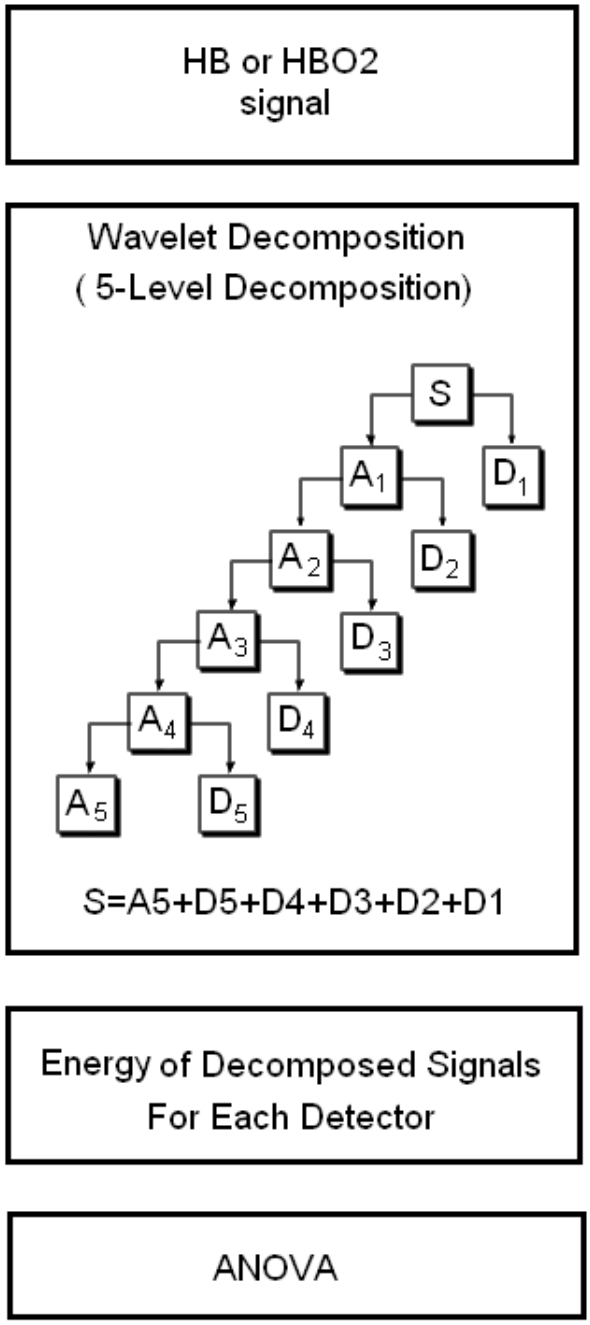

Figure 5.7 Signal Processing Algorithm.

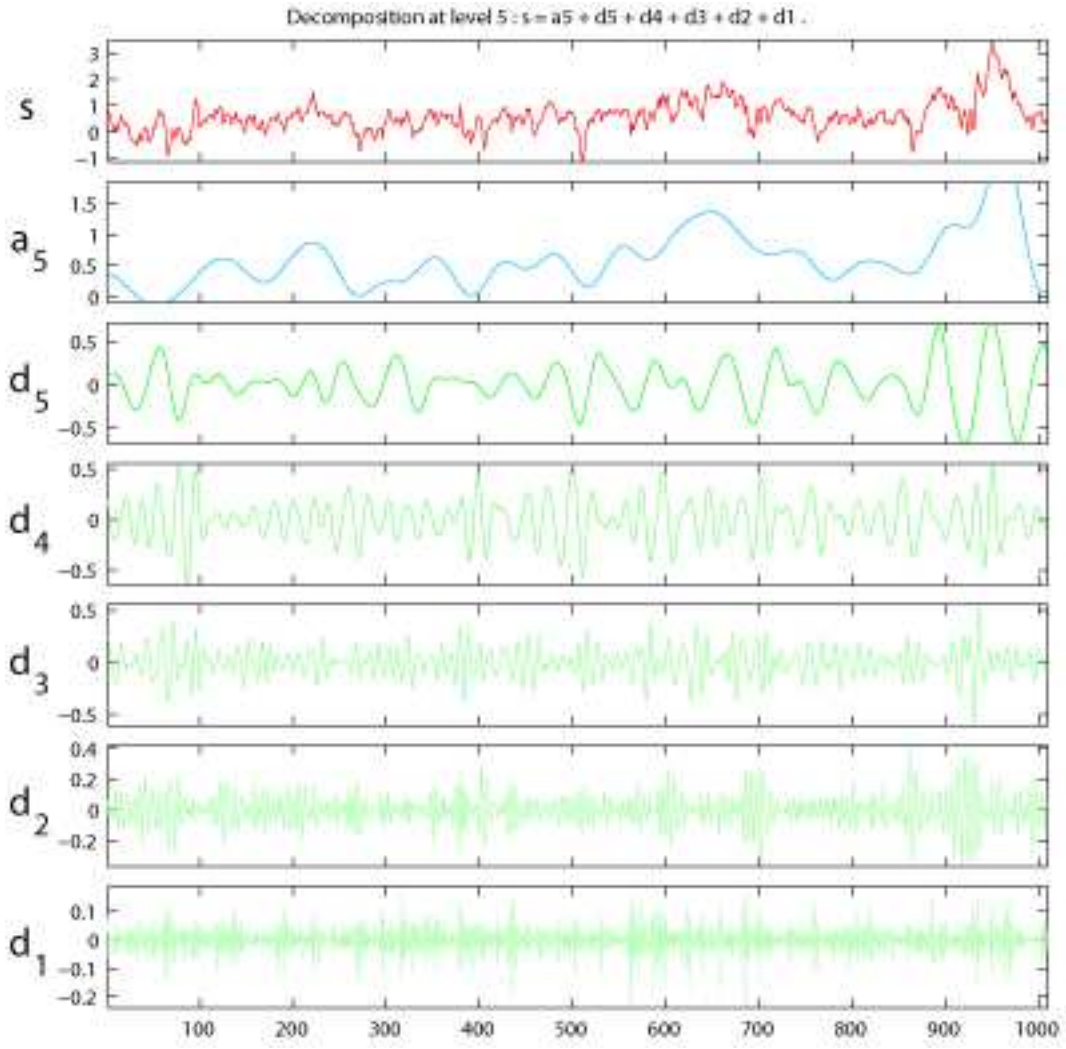

Figure 5.8 Decomposed Signals.

on forehead. The corresponding Figures of spectral analysis and wavelet decomposition are shown in Appendix D and E.

6. RESULTS AND DISCUSSION

6.1 Behavioral Results

In several, schizophrenia patients have poor performance on cognitive tasks. Therefore, we expect increased reaction times and higher error rates. Table 6.1 shows the mean and standard deviation of the reaction times and error rates of control and schizophrenic group. Reaction times were calculated as the average of only correct answers. The results show that the reaction times increase from neutral to incongruent trials in both group. Furthermore, the mean reaction times of schizophrenic group are higher than the control group as shown in Figure 6.1. The standard deviations of healthy group are higher. Also, ANOVA results show that response time of schizophrenic patients is significantly longer than the response time of control subjects for neural, congruent and incongruent trials ($p<0.05$). The mean error rates of schizophrenic patients are higher than that of control group as shown in Figure 6.2. The standard deviations of schizophrenic patients are higher. However, for only incongruent trials, error rates of schizophrenic patients are significantly different ($p<0.05$).

To sum up, schizophrenia patients were slower than controls under three conditions (neutral, congruent and incongruent) as expected. Also, their results were faultier than controls.

6.2 NIRS Results

The concentration changes of oxy-Hb and deoxy-Hb signals were observed during the Stroop task. The Stroop task was used because it shown to activate the frontal lobe regions which is accessible with fNIRS systems. According to most of the researchers, there is a hypofunctionality of the frontal lobes of schizophrenic patients. Therefore, a decrease in signal energies of schizophrenic patients was expected in this study.

Table 6.1
Reaction Times and Error Rates for Stroop Task.

	Healthy Control Participants		**Schizophrenia Patients**		**ANOVA Results**	
	Mean	**Std**	**Mean**	**Std**	**F Value**	**P Value**
Reaction Times						
Neutral	0.98	0.45	1.75	0.14	33.27	1.29e-6, $p<0.05$
Congruent	1.05	0.32	1.81	0.19	56.14	6.31e-9, $p<0.05$
Incongruent	1.18	0.34	2.20	0.24	88.31	2.43e-11, $p<0.05$
Error Rates						
Neutral	0.02	0.02	0.08	0.14	2.71	0.1083
Congruent	0.03	0.05	0.10	0.13	3.01	0.0912
Incongruent	0.07	0.08	0.30	0.21	13.03	0.0009, $p<0.05$

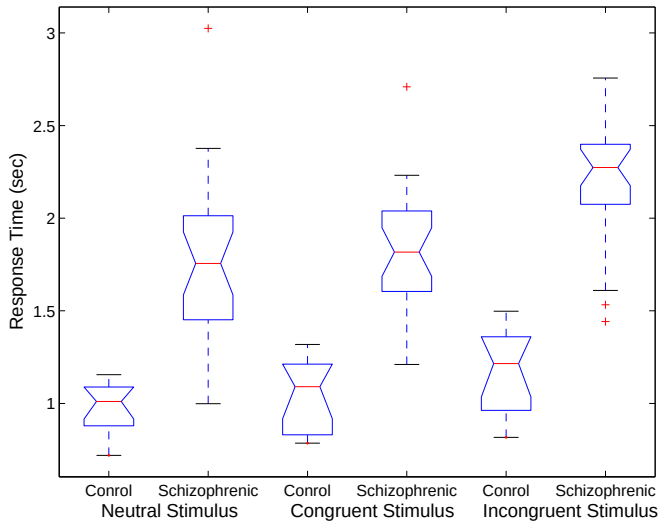

Figure 6.1 Response Times of Schizophrenic Patients and Healthy Controls.

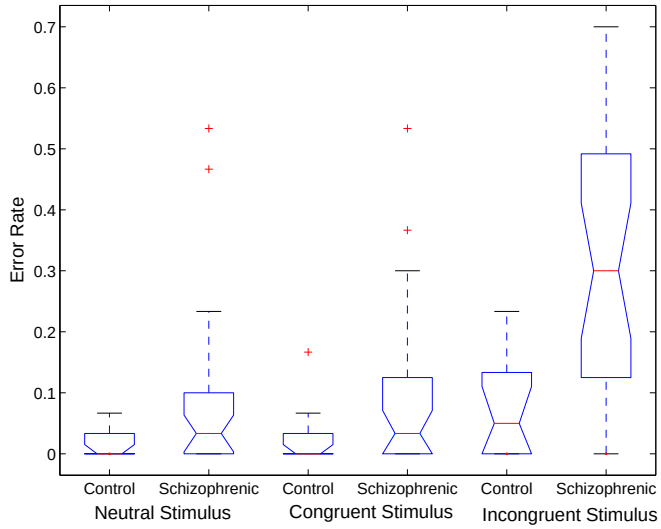

Figure 6.2 Error Rates of of Schizophrenic Patients and Healthy Controls.

In the first section, we analyzed fNIRS data with spectral analysis method. Energies of oxy-Hb and deoxy-Hb signals for neutral, congruent and incongruent trials were calculated in very low, low and high frequency regions. Anova test was used to show the energies of schizophrenic and control group are significantly different. White regions in Figures 6.3, 6.4 and 6.5 show that the energies of the schizophrenic patients and control subjects are statistically different and black regions show that there is no such difference. The detectors 1, 2, 3, and 4 correspond to left region of the brain. The detectors 5, 6, 7, and 8 cover mid-left region ,and 9, 10, 11 and 12 cover mid-right region. The detectors 13-14-15-16 correspond to right region.

As understood from the figures, there are more detectors at which changes in oxy-Hb are more significantly. For oxy-Hb signals, controls have higher energy at left region of the frontal cortex in low and very low frequency bands during neutral trials. During congruent trials, energy of controls is higher at left region of the frontal cortex in very low frequency band, and there is a bilateral activation in low frequency band. For incongruent trials, mid-left region is more activated in very low frequency band, and right and left regions are more activated in low frequency band. In high frequency band, there are very few detectors at which the deoxy-Hb and oxy-Hb signals are significantly different.

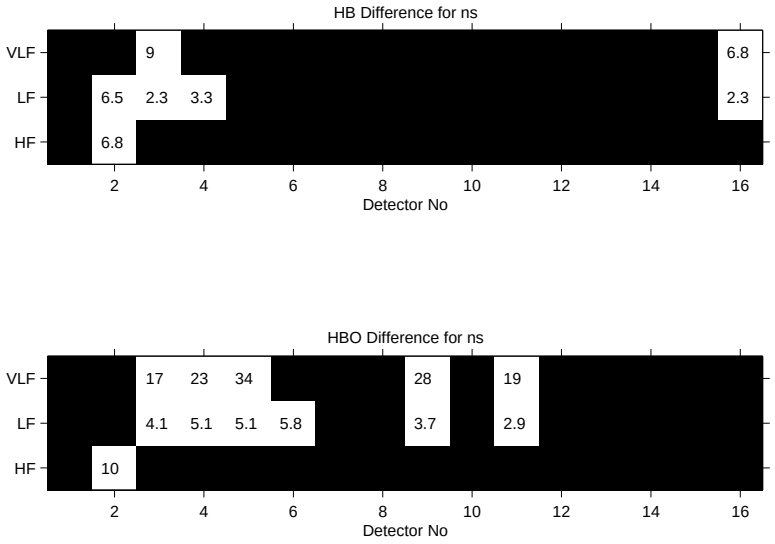

Figure 6.3 Anova Results for Neutral Stimulus.

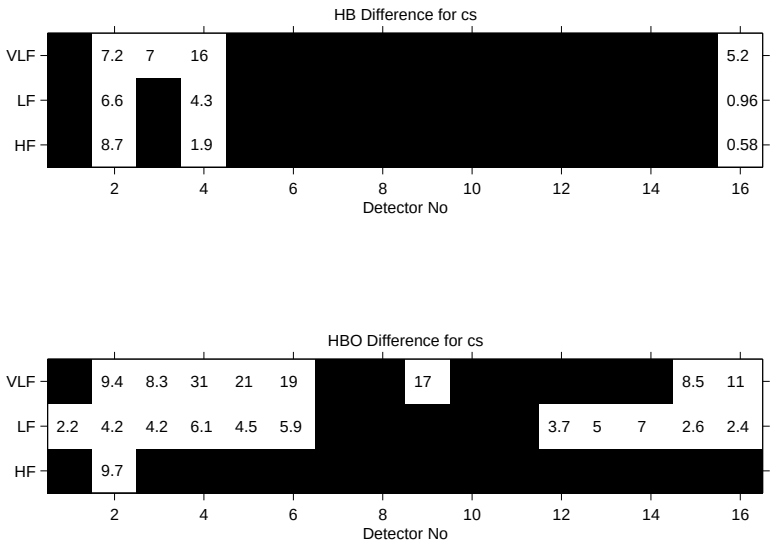

Figure 6.4 Anova Results for Congruent Stimulus.

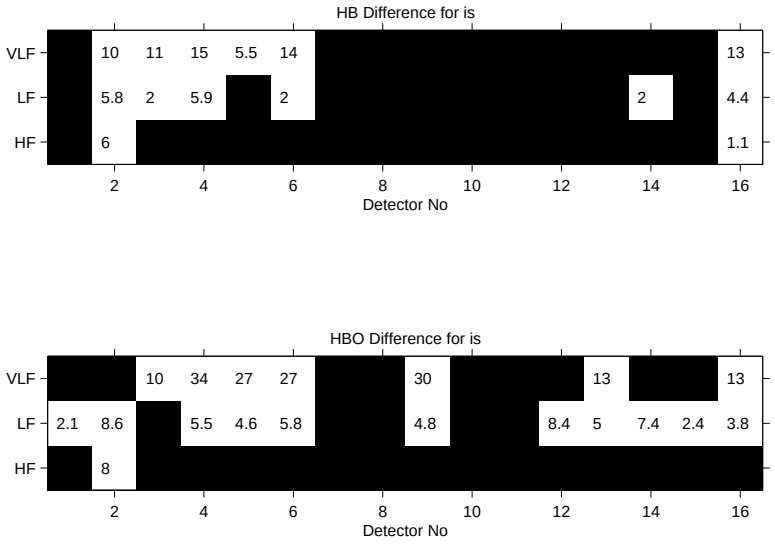

Figure 6.5 Anova Results for Incongruent Stimulus.

The following figures demonstrate the deoxy-Hb difference during incongruent trials in very low and low frequency bands more clearly (Fig 6.6, 6.7,and 6.8). Activation is increasing from dark blue to red.

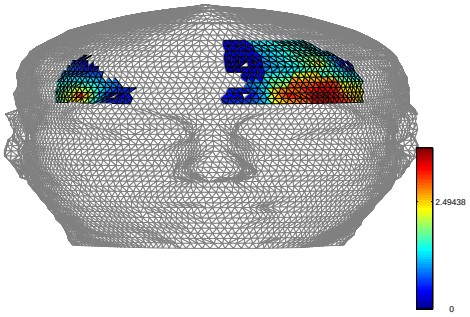

Figure 6.6 Very low frequency-HB-Incongruent.

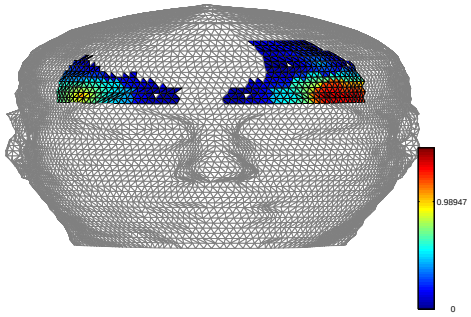

Figure 6.7 Low frequency-HB-Incongruent.

In the second part of the thesis, wavelet decomposition of fNIRS data was performed. After five level wavelet decomposition of deoxy-Hb and oxy-Hb signals with Daubechies 10, the energies of each detector in each subband were calculated. The figures C.1 to C.12 show the energies of decomposed oxy-Hb and deoxy-Hb signals for neural, congruent and incongruent situations. In decomposed deoxy-Hb signals, the changes are not distinguishable with eye. On the other hand, decomposed oxy-Hb signals are noticeable especially in A5 band.

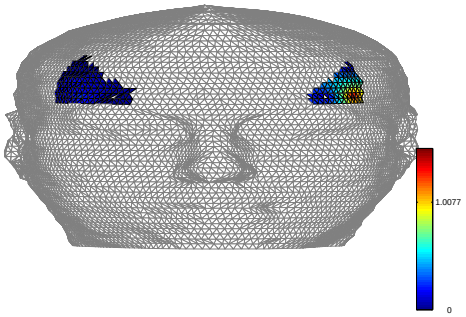

Figure 6.8 High frequency-HB-Incongruent.

We applied one way ANOVA test in order to find at which detectors the energies of schizophrenia patients and control subjects are statistically different. As in the first section, white regions in Figures 6.9, 6.10 and 6.11 show that the energies of the schizophrenic patients and control subjects are statistically different.

There are no changes in decomposed deoxy-Hb signals except for a few detectors, as shown in Figure 6.9. However, the decomposed oxy-Hb signal of schizophrenic patients is significantly different from that of control subjects in almost all detectors in A5 frequency band (detectors 2, 4, 5, 6, 7, 9, 11, 12, 13, 15 and 16).

In the case of congruent situation, the energy of the schizophrenic group is less than control group in right and mid-left region in A5 frequency band (detectors 2, 5, 7, 9, 11, 12, 13, 14, 15, and 16).

At detectors 2, 4, 5, 6, 7, 9, 11, 12, 13, 15, and 16, there is a significant difference in terms of energies of oxy-HB and deoxy-Hb signals in A5 band.

The results of ANOVA show that energies of schizophrenic patients are lower than energies of control subjects in low frequency band (A5 band). Also, there is a significant difference in D1 band. However, we do not know how to explain these result since this frequency band corresponds to Fs/4, Fs/2Hz and sampling frequency is about 1.7 Hz. We do not expect significant changes in very high frequency band.

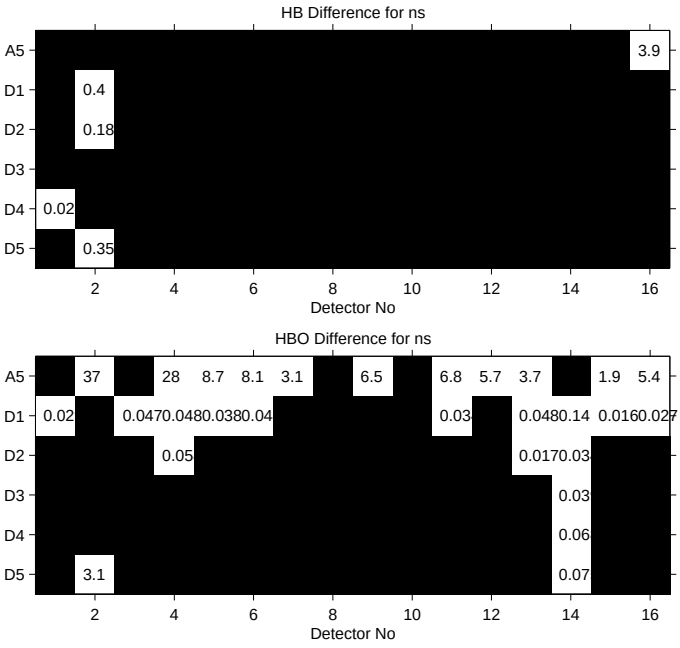

Figure 6.9 Anova Results for Neutral Stimulus.

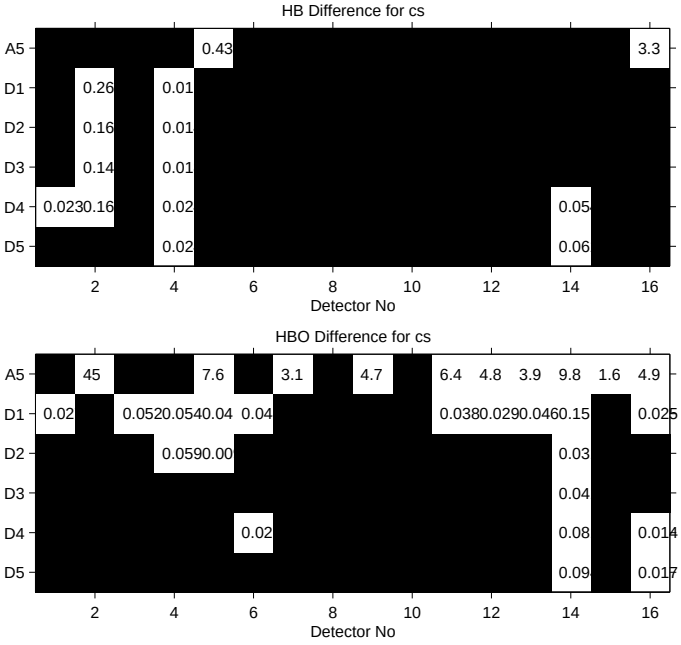

Figure 6.10 Anova Results for Congruent Stimulus.

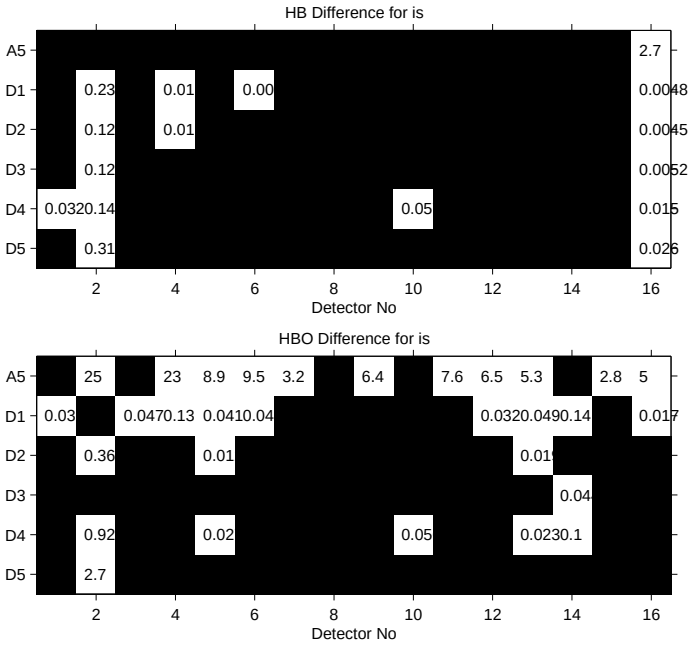

Figure 6.11 Anova Results for Incongruent Stimulus.

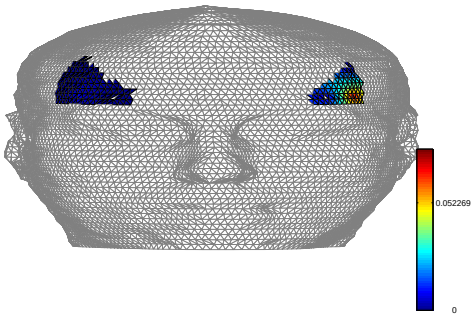

Figure 6.12 D5 band-HB-Incongruent.

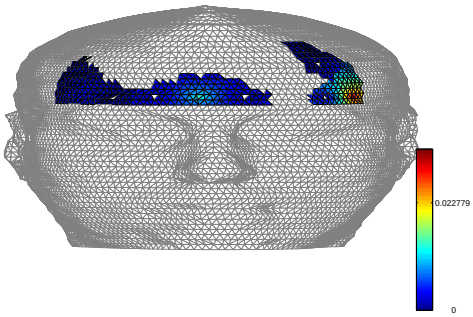

Figure 6.13 D4 band-HB-Incongruent.

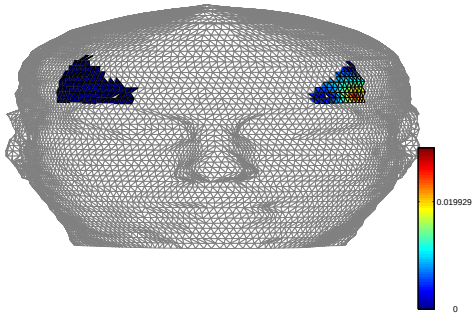

Figure 6.14 D3 band-HB-Incongruent.

7. CONCLUSION

In this study, functional near infrared spectroscopy is used to explore the differences of prefrontal cortex hemodynamics during Stroop task between schizophrenic patients and healthy control group. Twenty seven schizophrenic patients and twelve healthy control subjects were included in this study.

In literature, research conducted on schizophrenic patients shows that they have functional hypofrontality during the cognitive tasks. In our study, similar to others, the behavioral performance of schizophrenic patients on Stroop task were worse than the control group. Their response times are remarkably longer. Moreover, their error rates were higher than controls.

Frontal activation of schizophrenic patients and healthy control participants is investigated during Stroop task. After Oxy-Hb and deoxy-Hb changes were calculated, spectral analysis and 5-level wavelet decomposition was performed to these signals and energies of the decomposed signals were calculated for sixteen detectors. In both spectral analysis and wavelet decomposition method, the energy of schizophrenic patients is less than the energy of control subjects. This result is similar to the findings in literature. Furthermore, in spectral analysis, highly activated regions are mostly the left parts of the prefrontal cortex and the energy difference between the schizophrenic patients and control subjects is clearer in oxy-Hb signals. In the wavelet decomposition method, significantly reduced prefrontal activation in a group of schizophrenic patients as compared with healthy control group were found in very low frequency band (0 - 0.026 Hz) in mid-left, mid-right and right region of the brain. This result may indicate a specific hemodynamic response deficit within these regions of the cortex of schizophrenic patients.

As a conclusion, spectral analysis and wavelet decomposition appear suitable to observe the frontal activation in schizophrenic patients. Moreover, the wavelet decom-

position is more appropriate to explore the differences of hemodynamic responses in very precise subband regions.

APPENDIX A. The Modified Beer Lambert Law

In highly scattered medium such as brain, the oxy-Hb and deoxy-Hb concentration changes was calculated using modified beer lambert law. This law states that optical density (OD) is proportional to the concentration of deoxy-Hb (Hb), oxy-Hb (HbO_2) and the optical pathlength (L):

$$OD(\lambda_1) = \log[\frac{I_0(\lambda_1)}{I(\lambda_1)}] = \varepsilon_{HbO_2}(\lambda_1).[HbO_2].L + \varepsilon_{Hb}(\lambda_1).[Hb].L \tag{A.1}$$

$$OD(\lambda_2) = \log[\frac{I_0(\lambda_2)}{I(\lambda_2)}] = \varepsilon_{HbO_2}(\lambda_2).[HbO_2].L + \varepsilon_{Hb}(\lambda_2).[Hb].L \tag{A.2}$$

where I_0 is the received light intensity, I is the transmitted light intensity, λ_1 is wavelength1 and λ_2 is wavelength2. The oxy-Hb and deoxy-Hb changes in the brain can be calculated as follows:

$$\Delta OD(\lambda_1) = \varepsilon_{HbO_2}(\lambda_1).\Delta[HbO_2].L + \varepsilon_{Hb}(\lambda_1).\Delta[Hb].L \tag{A.3}$$

$$\Delta OD(\lambda_2) = \varepsilon_{HbO_2}(\lambda_2).\Delta[HbO_2].L + \varepsilon_{Hb}(\lambda_2).\Delta[Hb].L \tag{A.4}$$

$$\begin{pmatrix} \Delta OD(\lambda_1) \\ \Delta OD(\lambda_2) \end{pmatrix} = \begin{pmatrix} \varepsilon_{HbO_2}(\lambda_1) & \varepsilon_{Hb}(\lambda_1) \\ \varepsilon_{HbO_2}(\lambda_2) & \varepsilon_{Hb}(\lambda_2) \end{pmatrix} \begin{pmatrix} \Delta[HbO_2] \\ \Delta[Hb] \end{pmatrix} L \tag{A.5}$$

$$\begin{pmatrix} \Delta[HbO_2] \\ \Delta[Hb] \end{pmatrix} = \begin{pmatrix} \varepsilon_{HbO_2}(\lambda_1) & \varepsilon_{Hb}(\lambda_1) \\ \varepsilon_{HbO_2}(\lambda_2) & \varepsilon_{Hb}(\lambda_2) \end{pmatrix}^{-1} \begin{pmatrix} \Delta OD(\lambda_1) \\ \Delta OD(\lambda_2) \end{pmatrix} \frac{1}{L} \tag{A.6}$$

APPENDIX B. Energy Graphics of Frequency Band Analysis

Figures of Frequency Band Analysis

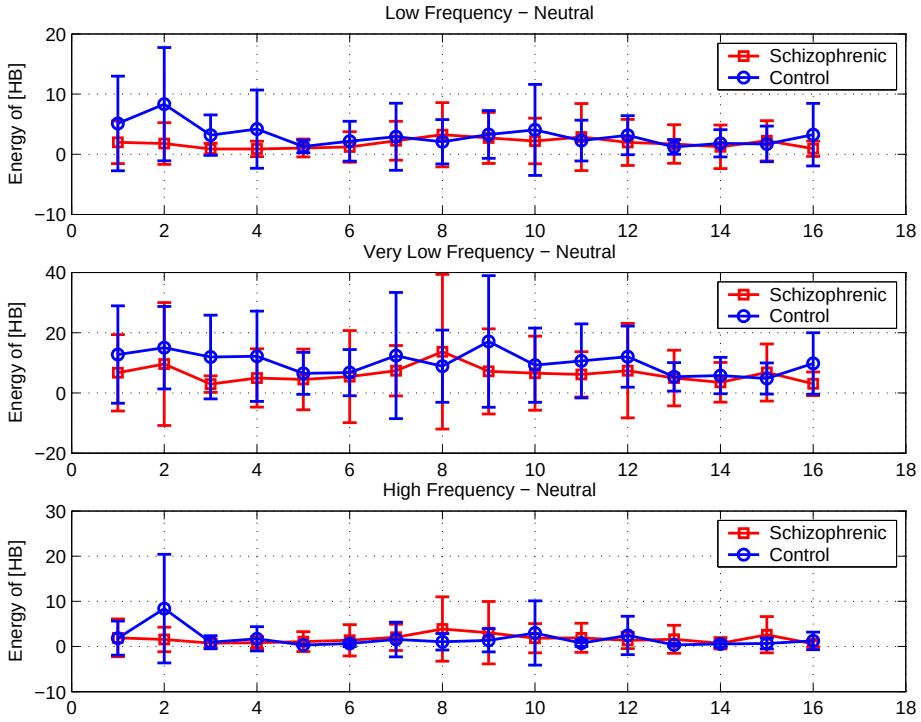

Figure B.1 HB signal for the neutral trials.

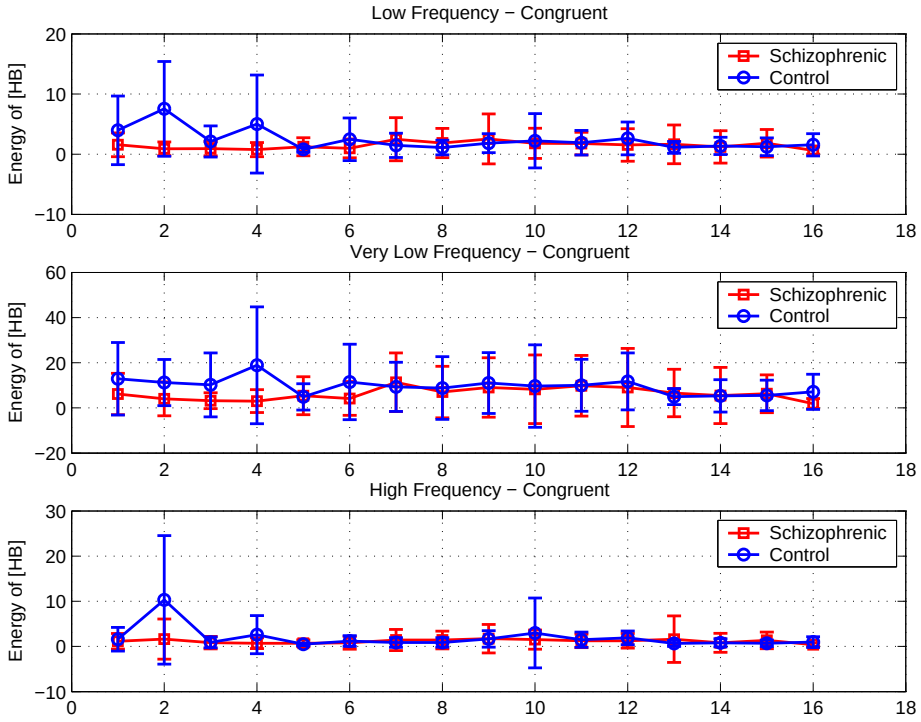

Figure B.2 HB signal for the congruent trials.

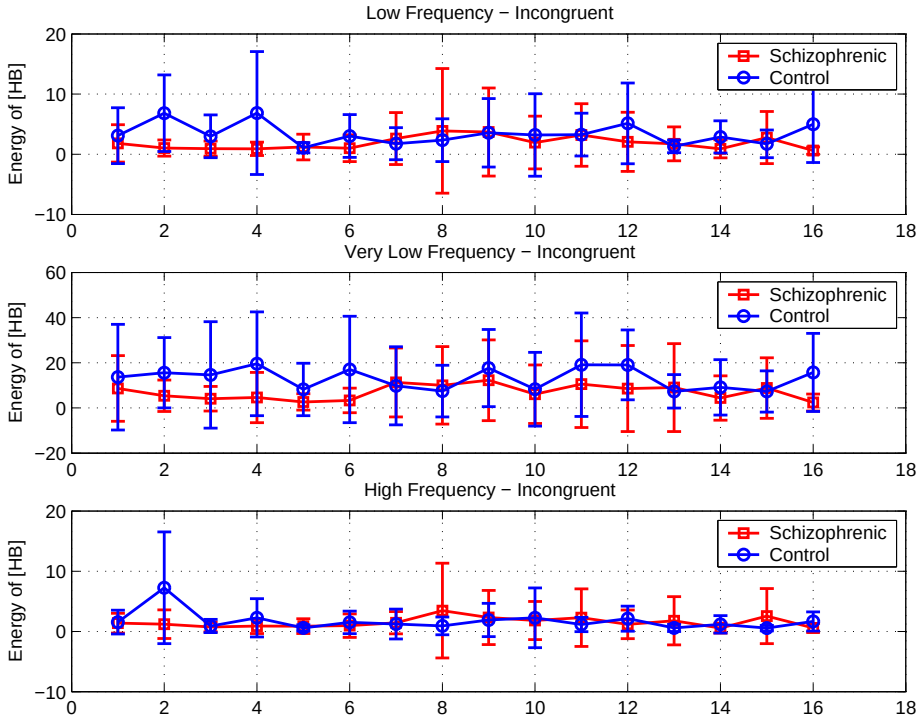

Figure B.3 HB signal for the incongruent trials.

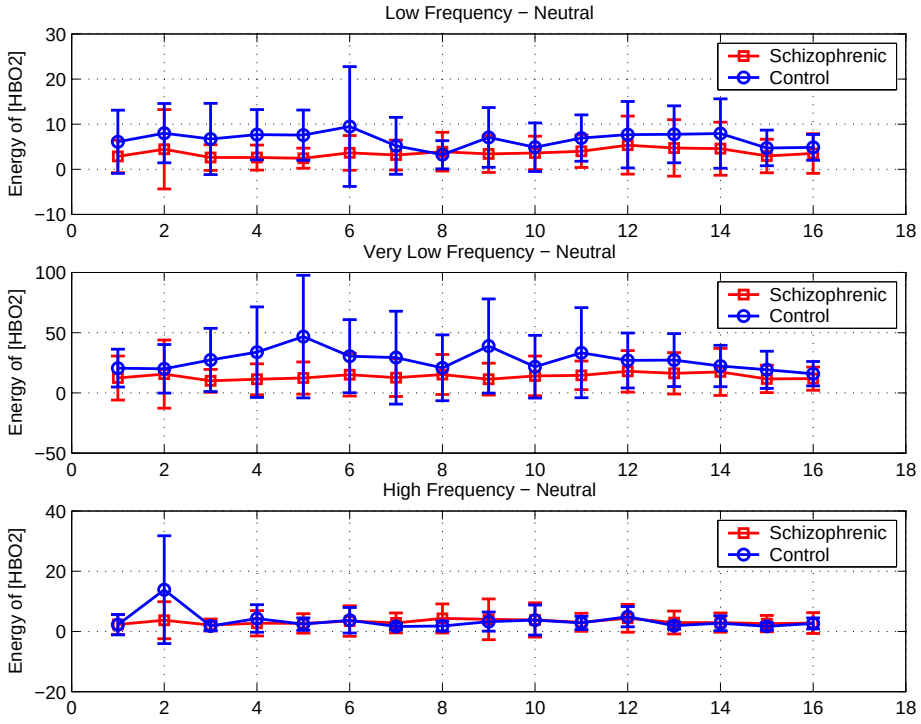

Figure B.4 HBO2 signal for the neutral trials.

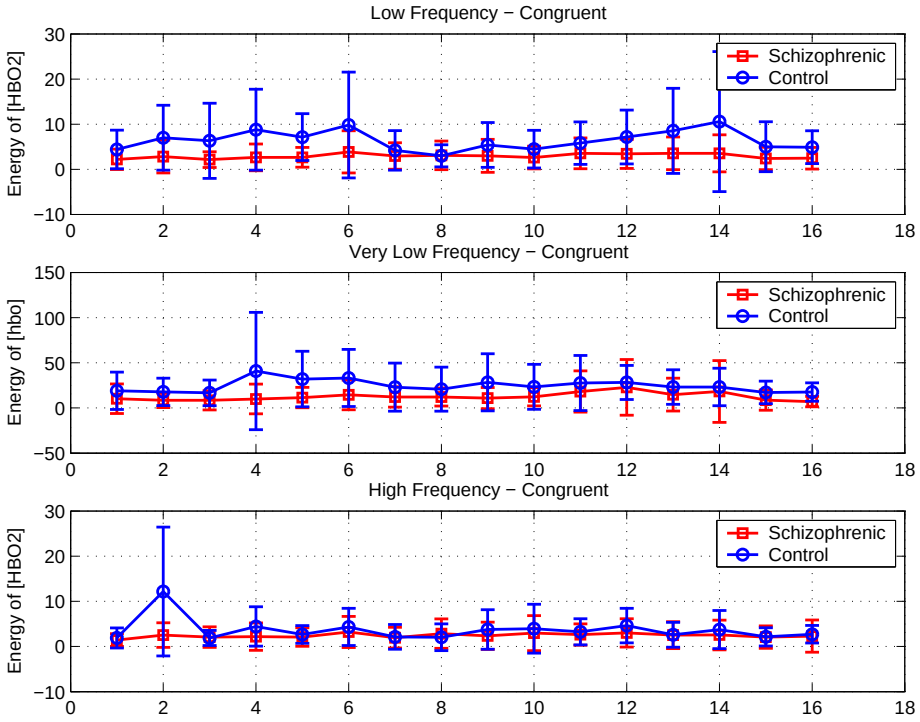

Figure B.5 HBO2 signal for the congruent trials.

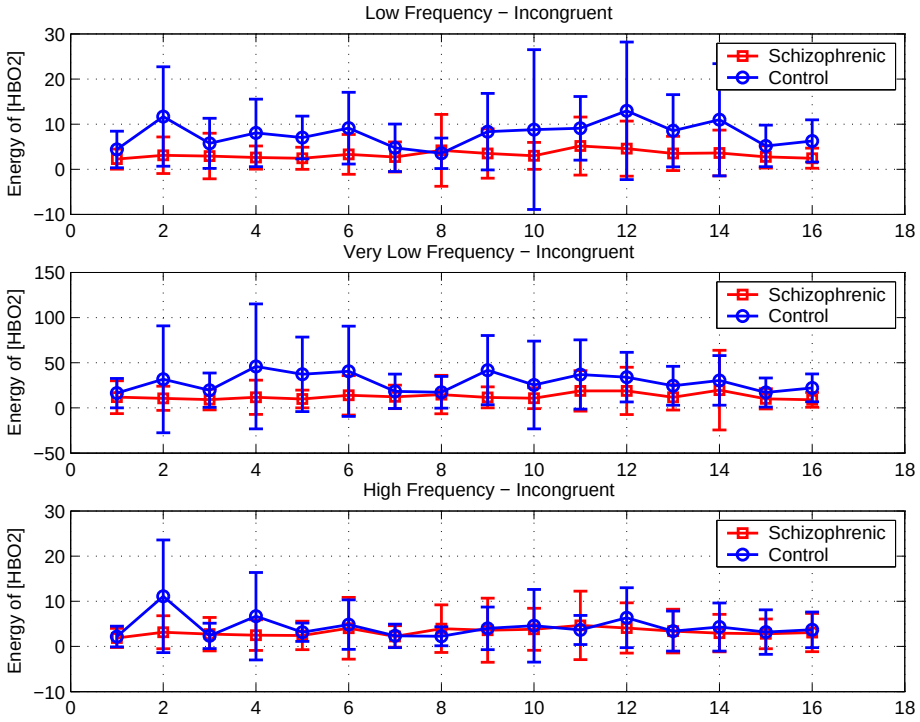

Figure B.6 HBO2 signal for the incongruent trials.

APPENDIX C. Energy Graphics of Wavelet Analysis

Figures of Frequency Band Analysis

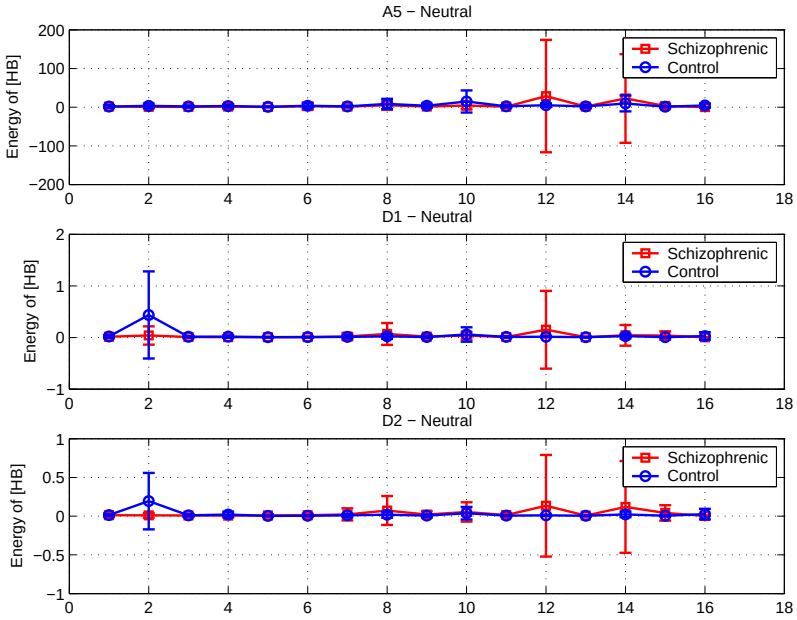

Figure C.1 Energy of deoxy-Hb signal for neutral stimulus in A5, D1, and D2 bands.

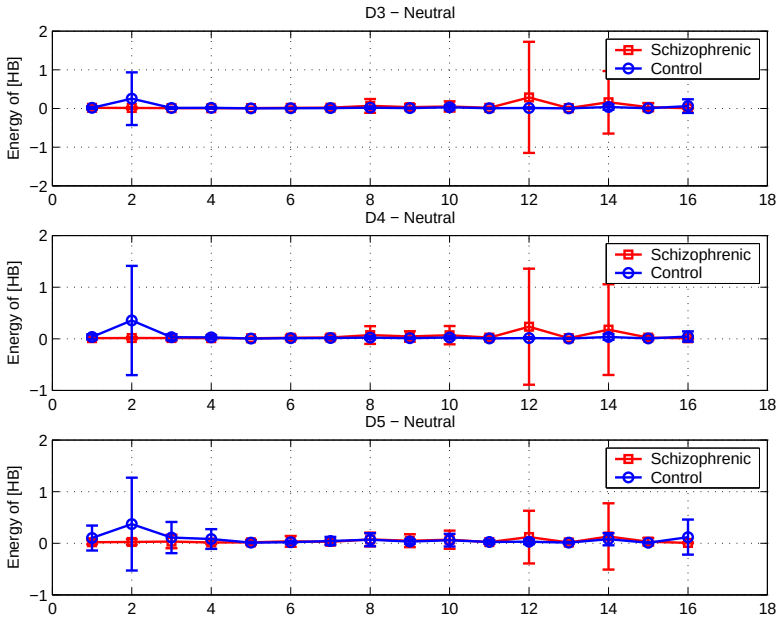

Figure C.2 Energy of deoxy-Hb signal for neutral stimulus in D3, D4, and D5 bands.

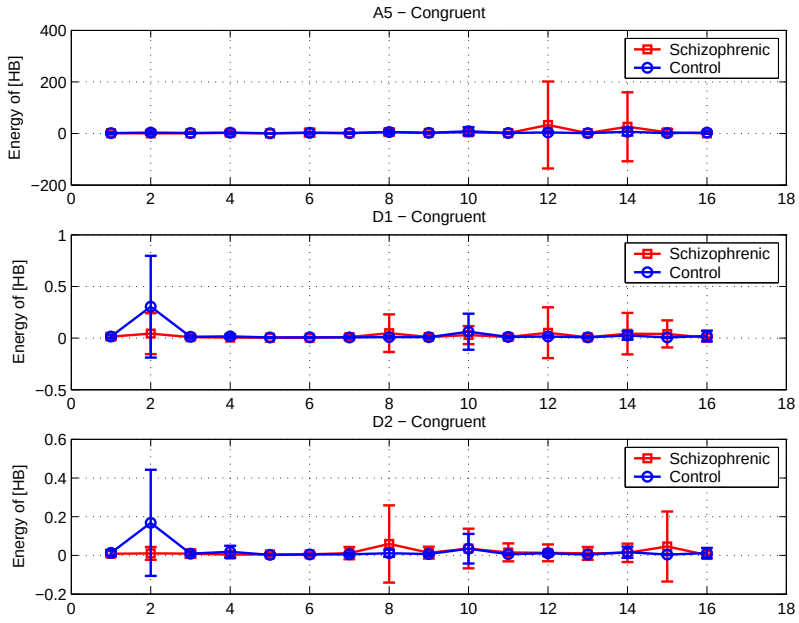

Figure C.3 Energy of deoxy-Hb signal for congruent stimulus in A5, D1, and D2 bands.

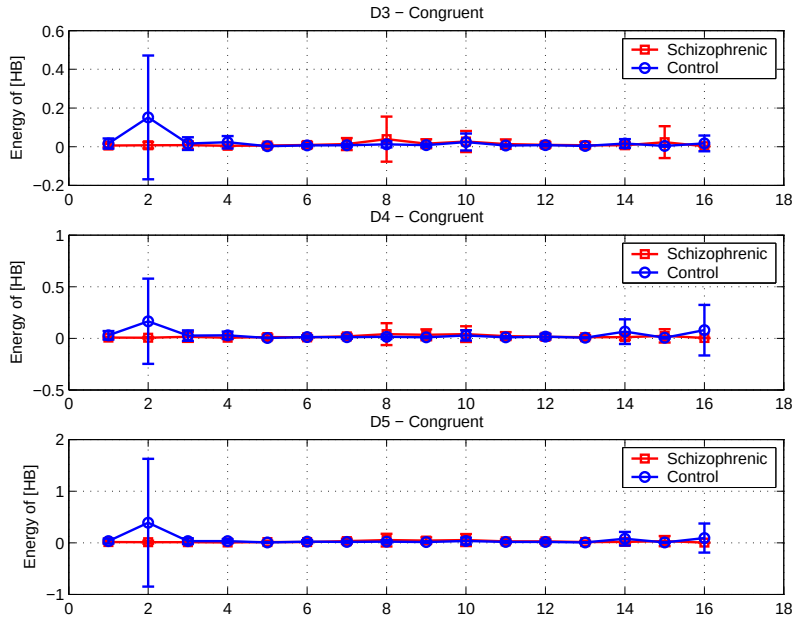

Figure C.4 Energy of deoxy-Hb signal for congruent stimulus in D3, D4, and D5 bands.

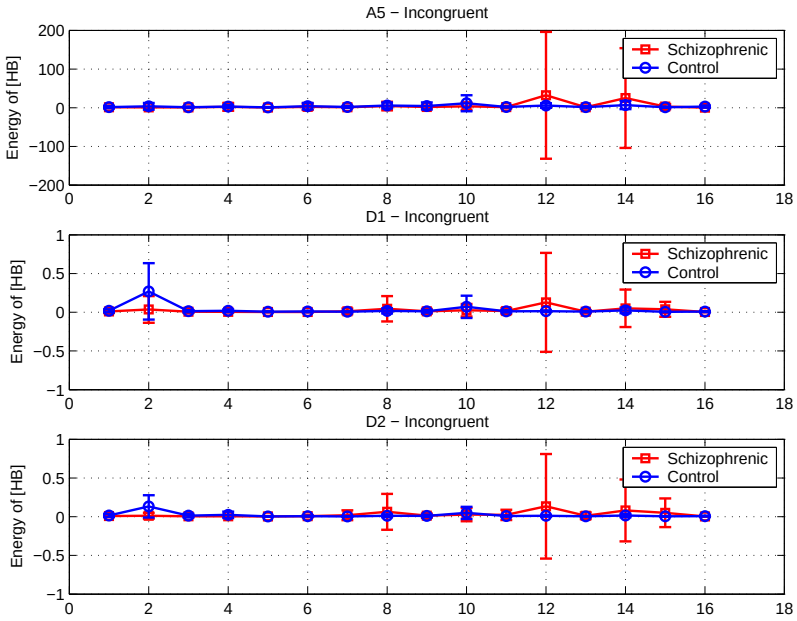

Figure C.5 Energy of deoxy-Hb signal for incongruent stimulus in A5, D1, and D2 bands.

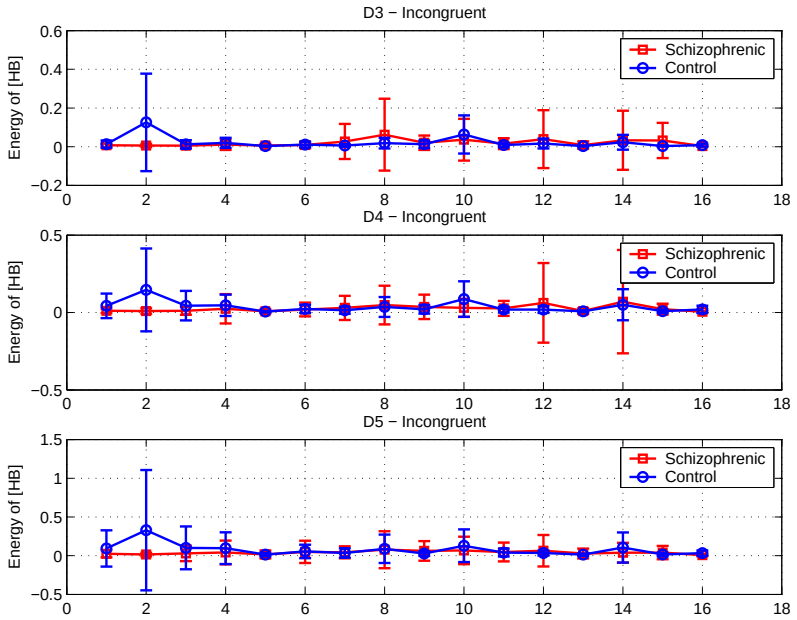

Figure C.6 Energy of deoxy-Hb signal for incongruent stimulus in D3, D4, and D5 bands.

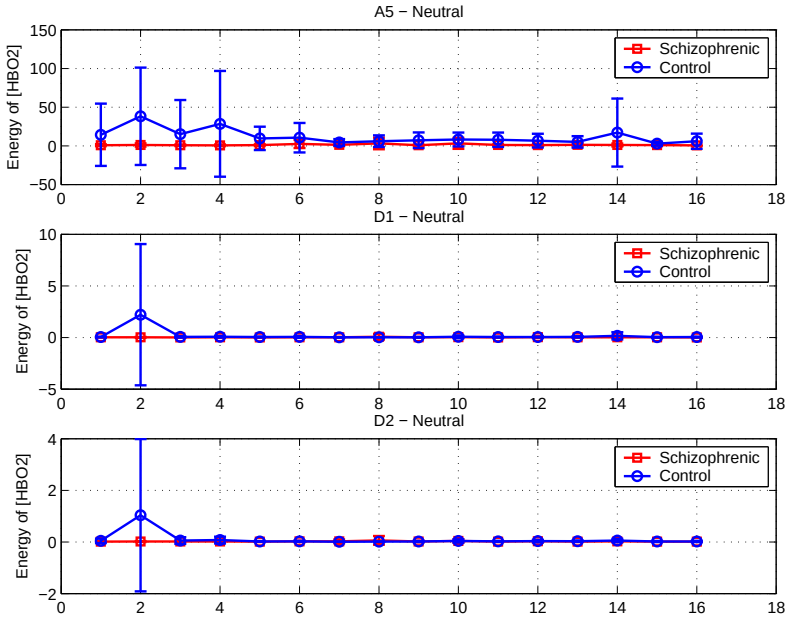

Figure C.7 Energy of oxy-Hb signal for neutral stimulus in A5, D1, and D2 bands.

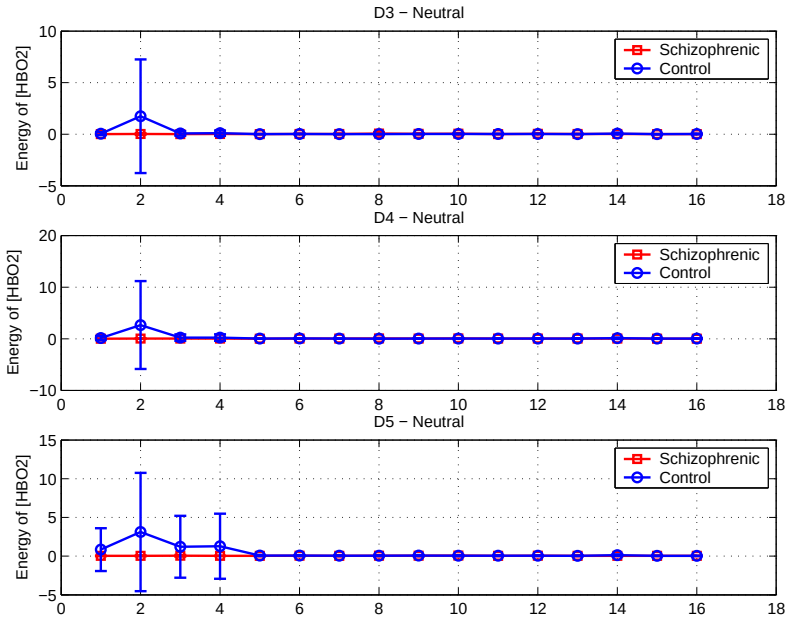

Figure C.8 Energy of oxy-Hb signal for neutral stimulus in D3, D4, and D5 bands.

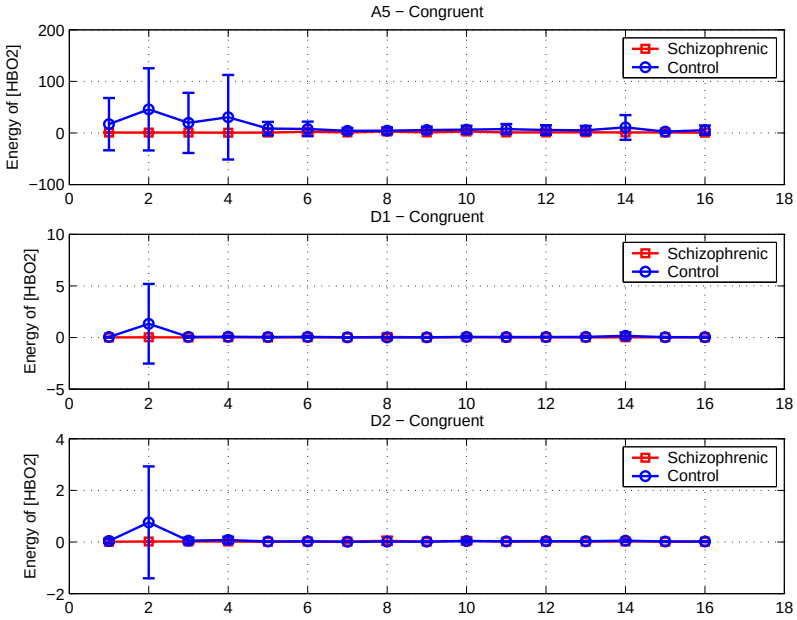

Figure C.9 Energy of oxy-Hb signal for congruent stimulus in A5, D1, and D2 bands.

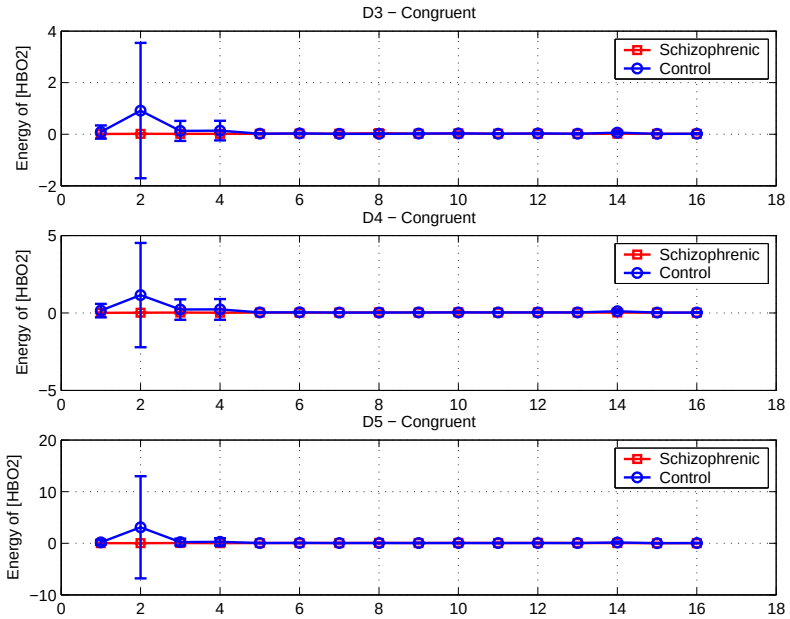

Figure C.10 Energy of oxy-Hb signal for congruent stimulus in D3, D4, and D5 bands.

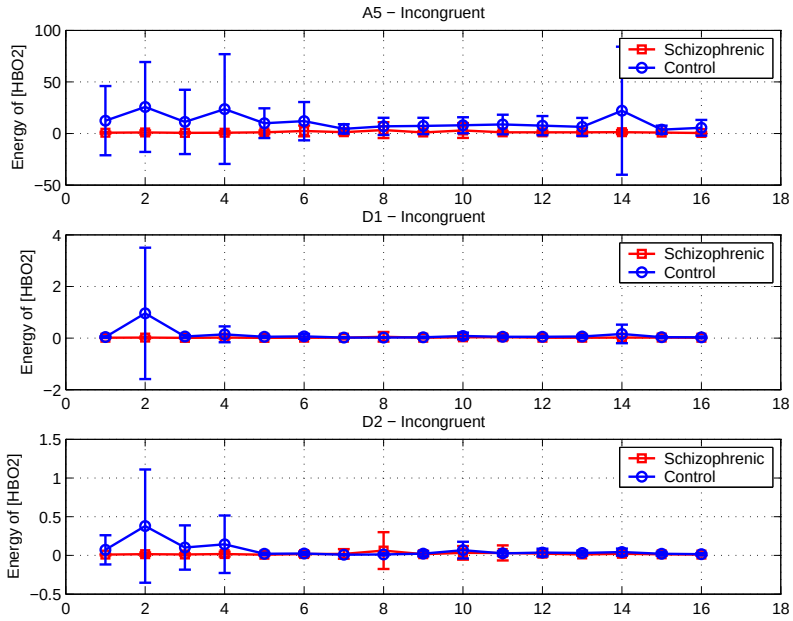

Figure C.11 Energy of oxy-Hb signal for incongruent stimulus in A5, D1, and D2 bands.

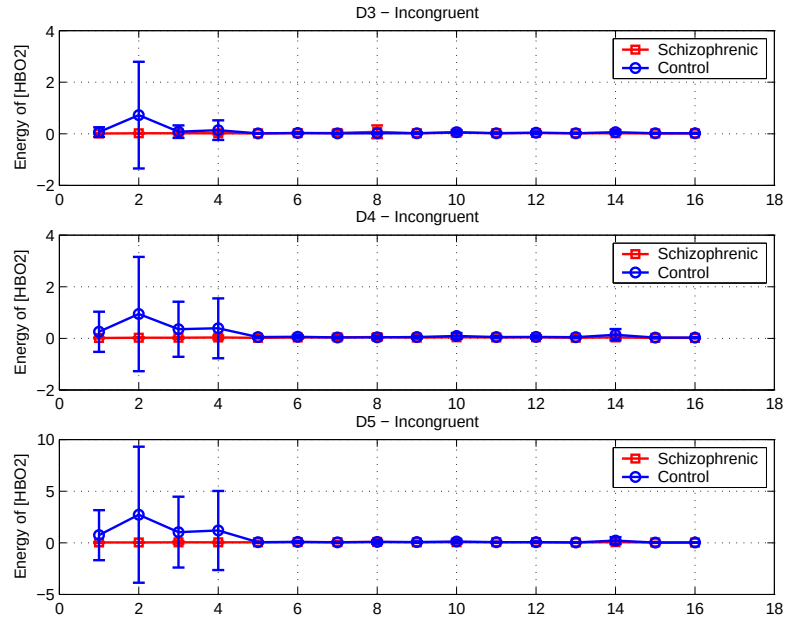

Figure C.12 Energy of oxy-Hb signal for incongruent stimulus in D3, D4, and D5 bands.

APPENDIX D. Activated Regions over Head Model - Frequency Band Analysis

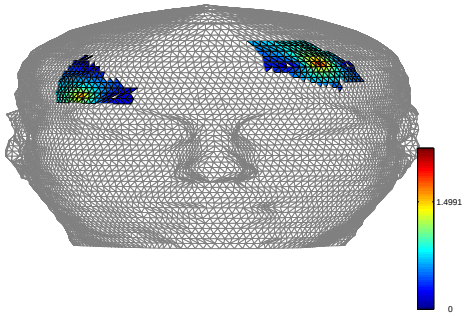

Figure D.1 Very low frequency-HB-Neutral.

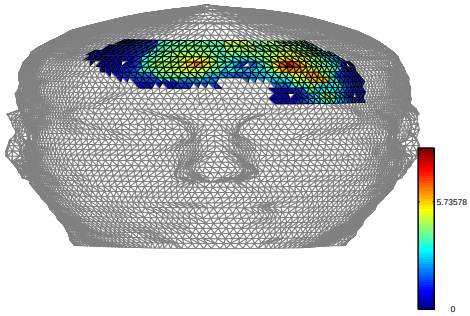

Figure D.2 Very low frequency-HBO2-Neutral.

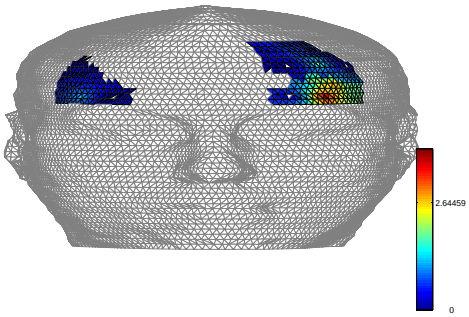

Figure D.3 Very low frequency-HB-Congruent.

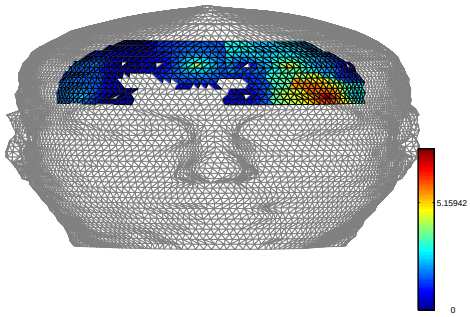

Figure D.4 Very Low frequency-HBO2-Congruent.

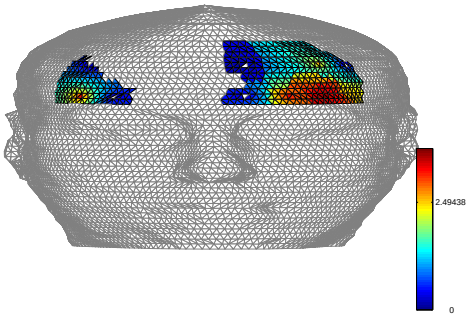

Figure D.5 Very low frequency-HB-Incongruent.

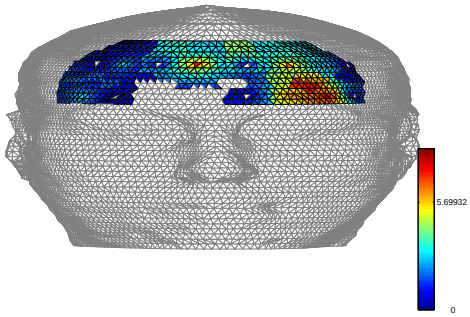

Figure D.6 Very low frequency-HBO2-Incongruent.

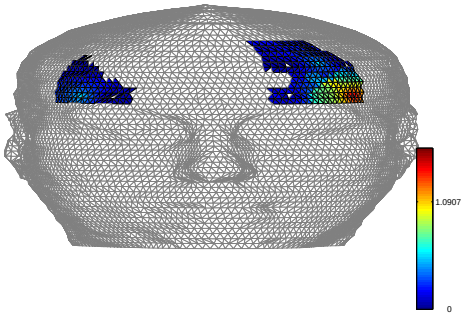

Figure D.7 Low frequency-HB-Neutral.

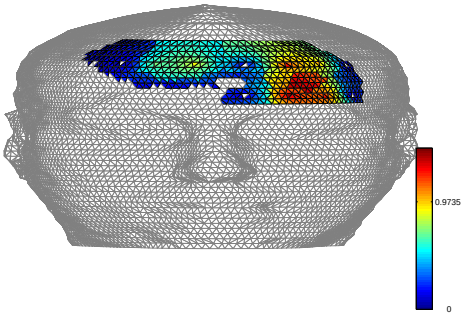

Figure D.8 Low frequency-HBO2-Neutral.

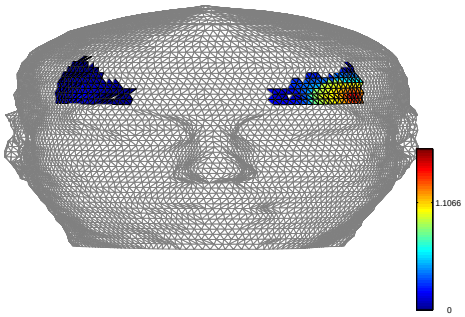

Figure D.9 Low frequency-HB-Congruent.

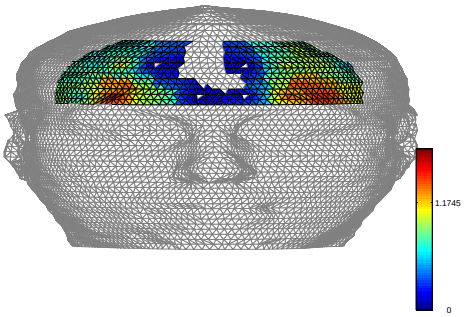

Figure D.10 Low frequency-HBO2-Congruent.

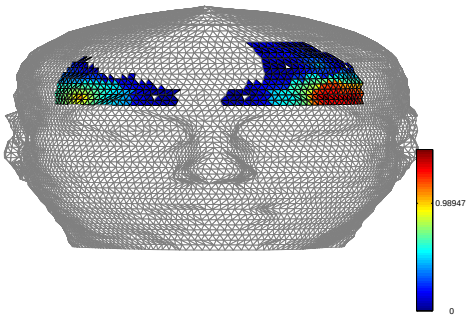

Figure D.11 Low frequency-HB-Incongruent.

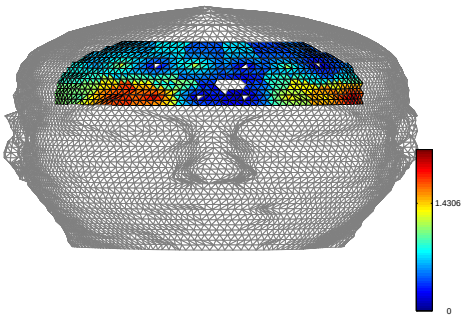

Figure D.12 Low frequency-HBO2-Incongruent.

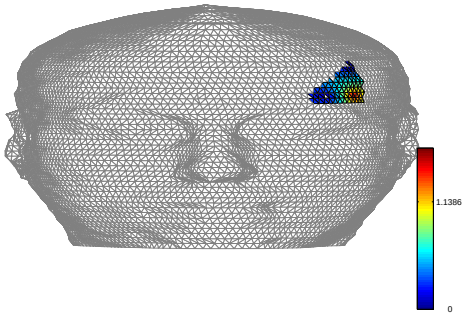

Figure D.13 High frequency-HB-Neutral.

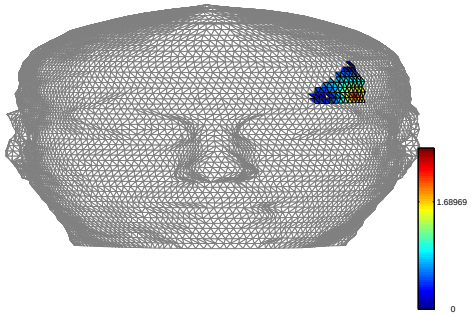

Figure D.14 High frequency-HBO2-Neutral.

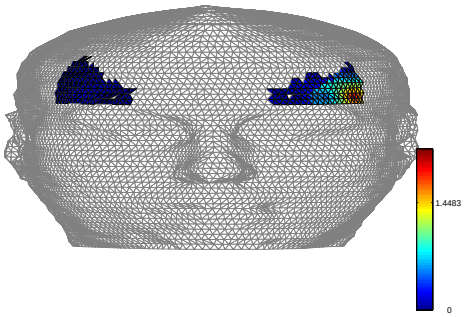

Figure D.15 High frequency-HB-Congruent.

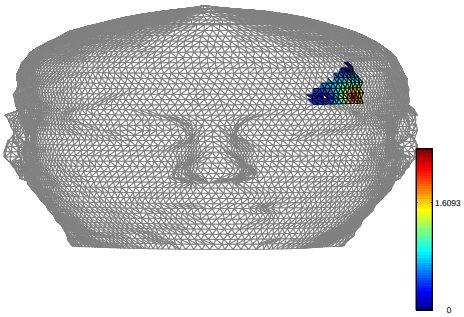

Figure D.16 High frequency-HBO2-Congruent.

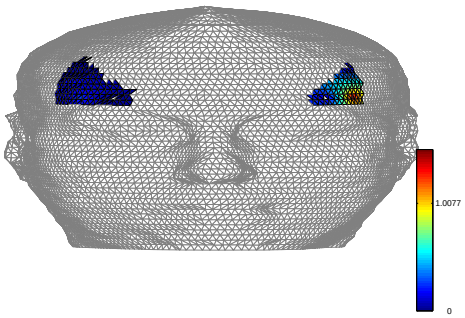

Figure D.17 High frequency-HB-Incongruent.

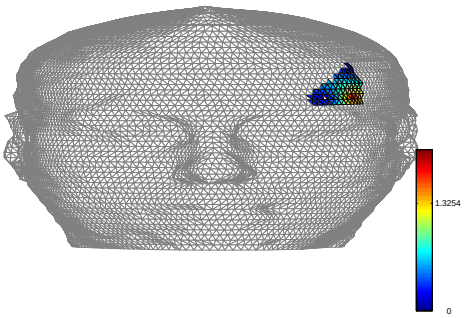

Figure D.18 High frequency-HBO2-Incongruent.

APPENDIX E. Activated Regions over Head Model - Wavelet Analysis

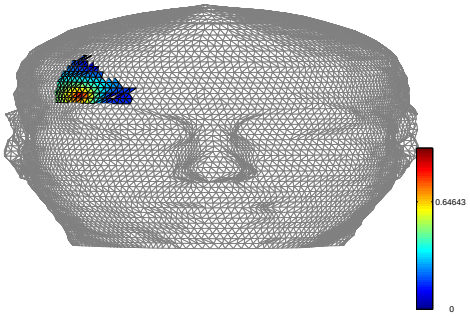

Figure E.1 A5 band-HB-Neutral.

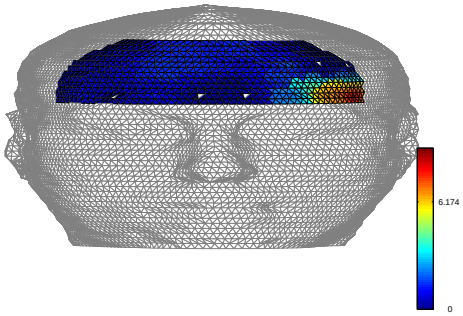

Figure E.2 A5 band-HBO2-Neutral.

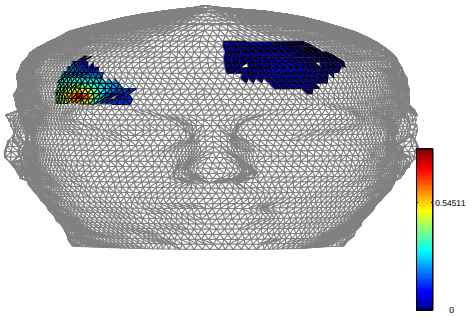

Figure E.3 A5 band-HB-Congruent.

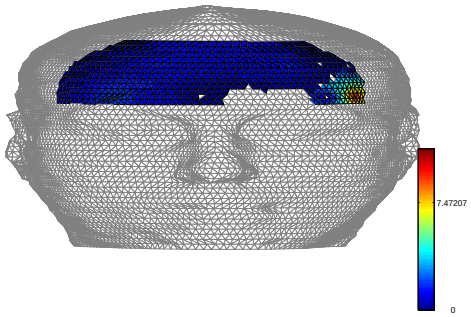

Figure E.4 A5 band-HBO2-Congruent.

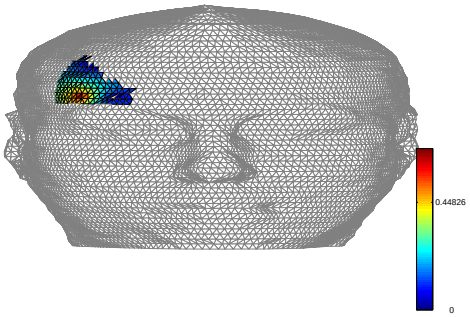

Figure E.5 A5 band-HB-Incongruent.

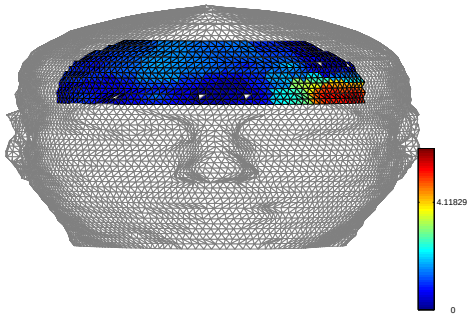

Figure E.6 A5 band-HBO2-Incongruent.

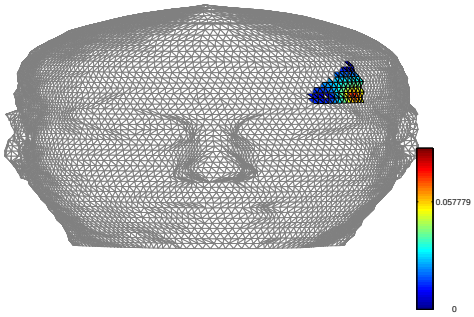

Figure E.7 D5 band-HB-Neutral.

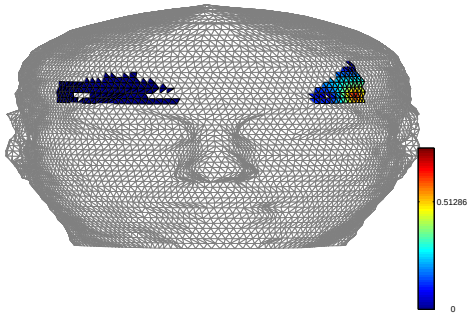

Figure E.8 D5 band-HBO2-Neutral.

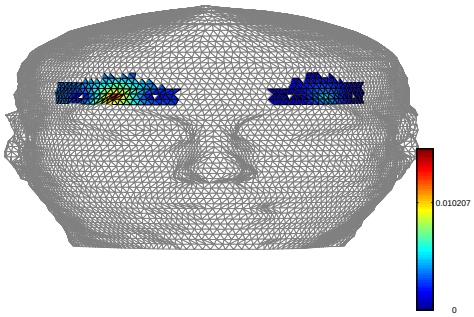

Figure E.9 D5 band-HB-Congruent.

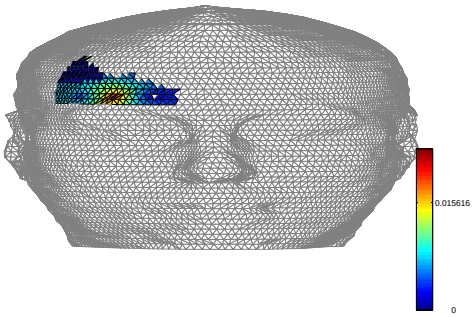

Figure E.10 D5 band-HBO2-Congruent.

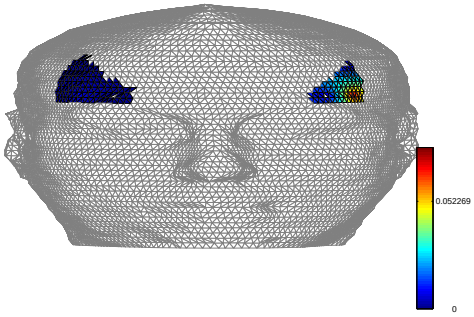

Figure E.11 D5 band-HB-Incongruent.

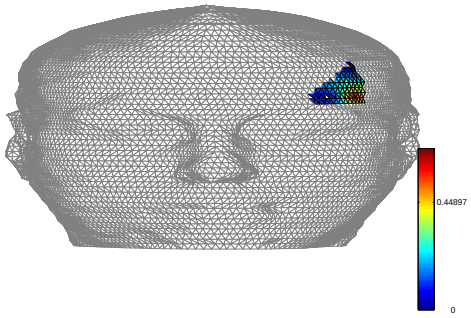

Figure E.12 D5 band-HBO2-Incongruent.

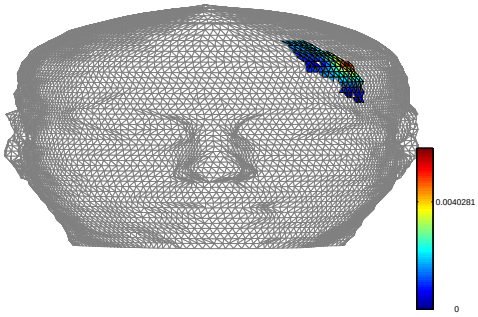

Figure E.13 D4 band-HB-Neutral.

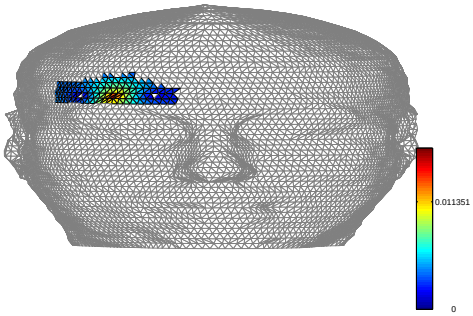

Figure E.14 D4 band-HBO2-Neutral.

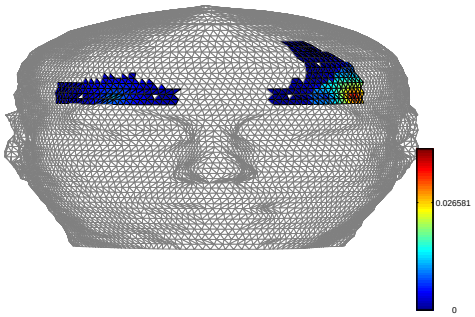

Figure E.15 D4 band-HB-Congruent.

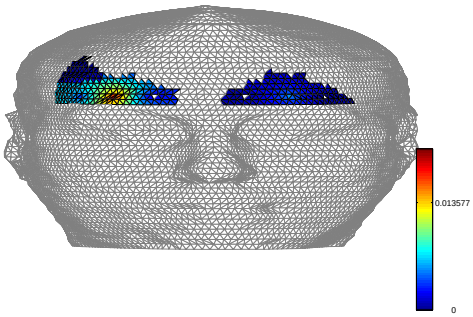

Figure E.16 D4 band-HBO2-Congruent.

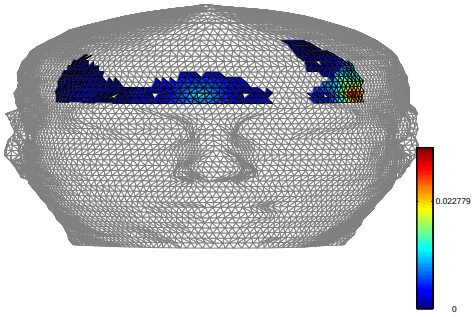

Figure E.17 D4 band-HB-Incongruent.

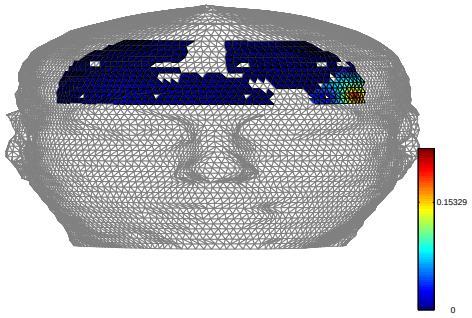

Figure E.18 D4 band-HBO2-Incongruent.

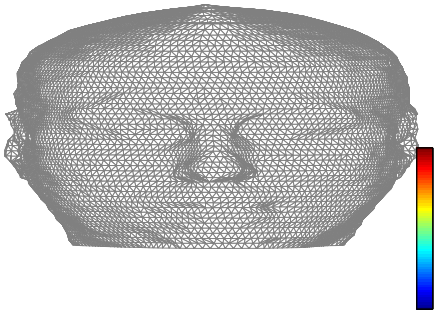

Figure E.19 D3 band-HB-Neutral.

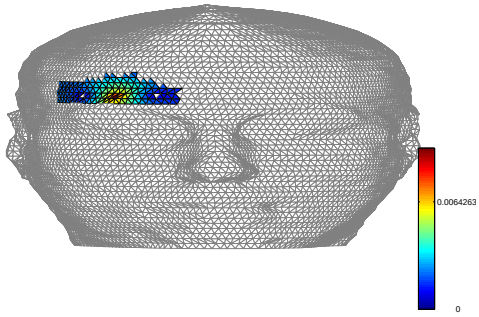

Figure E.20 D3 band-HBO2-Neutral.

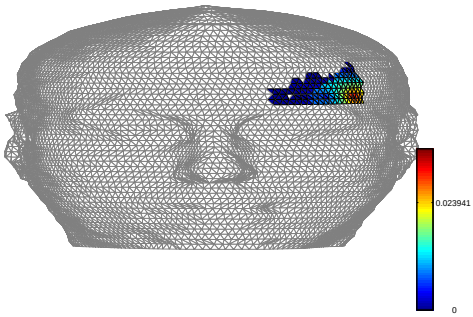

Figure E.21 D3 band-HB-Congruent.

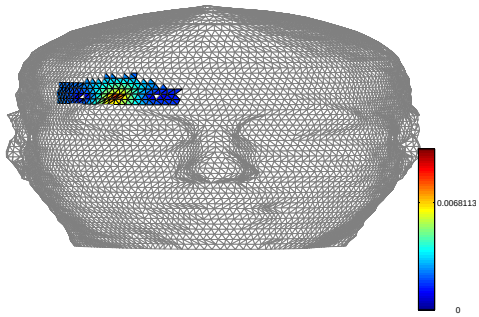

Figure E.22 D3 band-HBO2-Congruent.

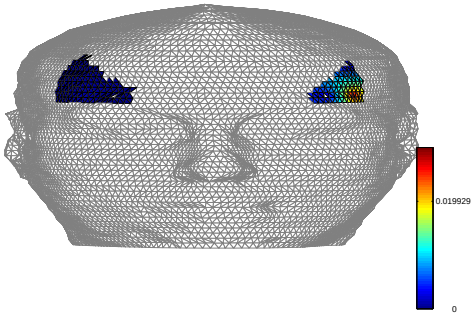

Figure E.23 D3 band-HB-Incongruent.

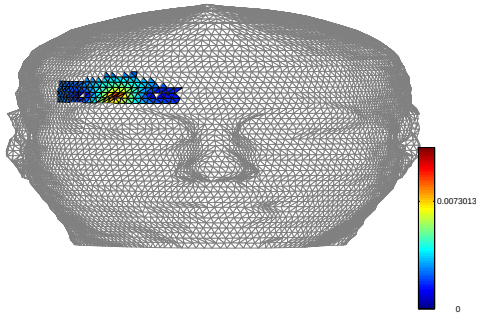

Figure E.24 D3 band-HBO2-Incongruent.

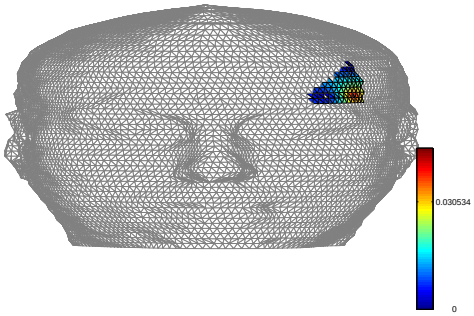

Figure E.25 D2 band-HB-Neutral.

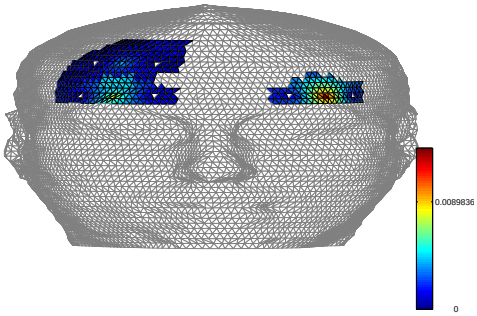

Figure E.26 D2 band-HBO2-Neutral.

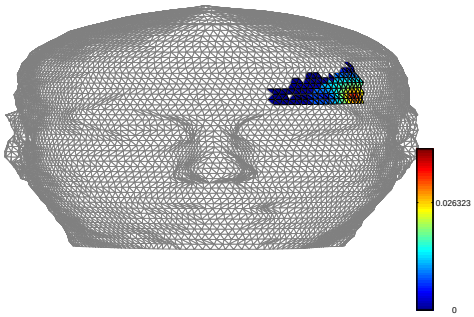

Figure E.27 D2 band-HB-Congruent.

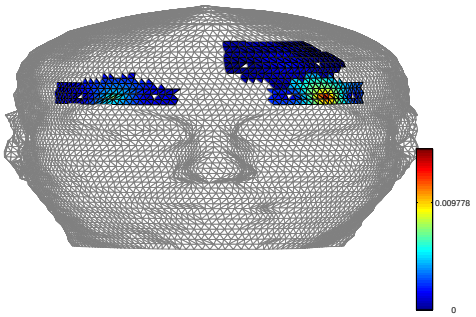

Figure E.28 D2 band-HBO2-Congruent.

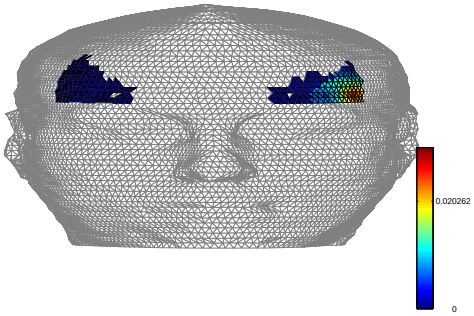

Figure E.29 D2 band-HB-Incongruent.

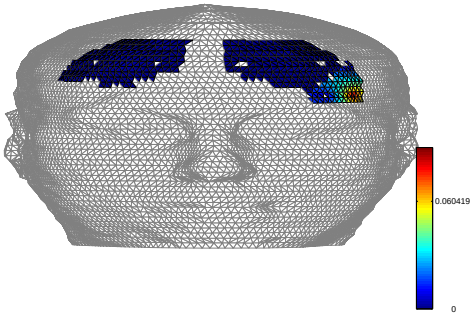

Figure E.30 D2 band-HBO2-Incongruent.

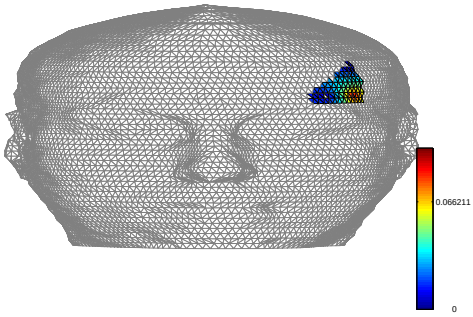

Figure E.31 D1 band-HB-Neutral.

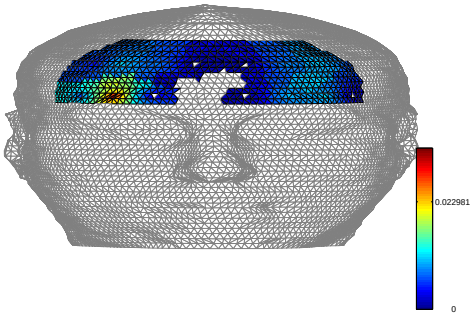

Figure E.32 D1 band-HBO2-Neutral.

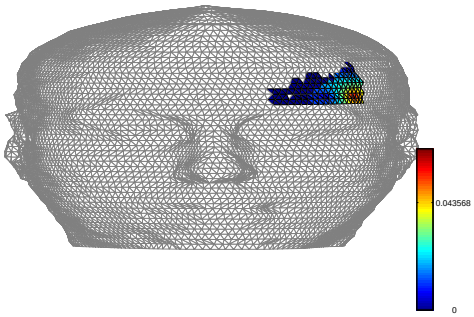

Figure E.33 D1 band-HB-Congruent.

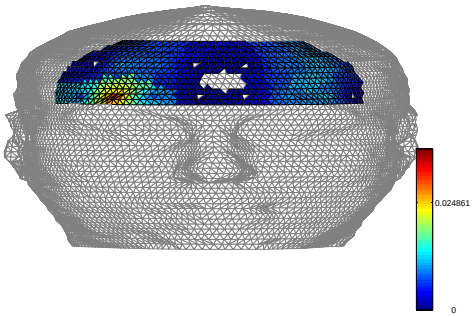

Figure E.34 D1 band-HBO2-Congruent.

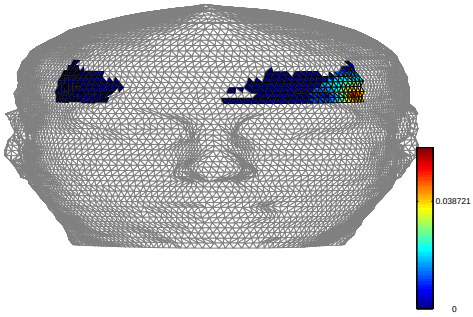

Figure E.35 D1 band-HB-Incongruent.

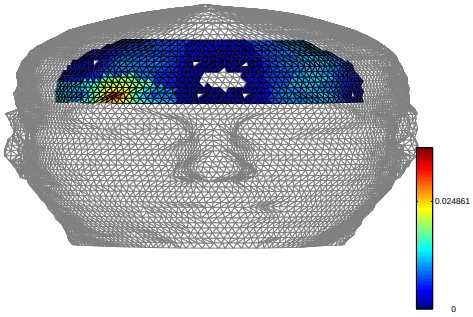

Figure E.36 D1 band-HBO2-Incongruent.

REFERENCES

1. Mark F. Bear, Barry W. Connors, M. A. P., *Neuroscience exploring the brain*, Lippincott Williams & Wilkins, second ed., 2001.

2. Eric R. Kandel, James H. Schwartz, T. M. J., *Principles of neural science*, Mc Graw Hill, fourth ed., 2000.

3. Fox, P. T., M. E. Raichle, M. A. Mintun, and C. Dence, "Nonoxidative glucose consumption during focal physiologic neural activity.," *Science*, Vol. 241, pp. 462–464, Jul 1988.

4. Bunce, S. C., M. Izzetoglu, K. Izzetoglu, B. Onaral, and K. Pourrezaei, "Functional near-infrared spectroscopy.," *IEEE Eng Med Biol Mag*, Vol. 25, no. 4, pp. 54–62, 2006.

5. Villringer, A., and B. Chance, "Non-invasive optical spectroscopy and imaging of human brain function.," *Trends Neurosci*, Vol. 20, pp. 435–442, Oct 1997.

6. Ehlis, A.-C., M. J. Herrmann, A. Wagener, and A. J. Fallgatter, "Multi-channel near-infrared spectroscopy detects specific inferior-frontal activation during incongruent stroop trials.," *Biol Psychol*, Vol. 69, pp. 315–331, Jul 2005.

7. Irani, F., S. M. Platek, S. Bunce, A. C. Ruocco, and D. Chute, "Functional near infrared spectroscopy (fnirs): an emerging neuroimaging technology with important applications for the study of brain disorders.," *Clin Neuropsychol*, Vol. 21, pp. 9–37, Jan 2007.

8. Shinba, T., M. Nagano, N. Kariya, K. Ogawa, T. Shinozaki, S. Shimosato, and Y. Hoshi, "Near-infrared spectroscopy analysis of frontal lobe dysfunction in schizophrenia.," *Biol Psychiatry*, Vol. 55, pp. 154–164, Jan 2004.

9. Manoach, D. S., "Prefrontal cortex dysfunction during working memory performance in schizophrenia: reconciling discrepant findings.," *Schizophr Res*, Vol. 60, pp. 285–298, Apr 2003.

10. Quintana, J., T. Wong, E. Ortiz-Portillo, E. Kovalik, T. Davidson, S. R. Marder, and J. C. Mazziotta, "Prefrontal-posterior parietal networks in schizophrenia: primary dysfunctions and secondary compensations.," *Biol Psychiatry*, Vol. 53, pp. 12–24, Jan 2003.

11. Ehlis, A.-C., M. J. Herrmann, M. M. Plichta, and A. J. Fallgatter, "Cortical activation during two verbal fluency tasks in schizophrenic patients and healthy controls as assessed by multi-channel near-infrared spectroscopy.," *Psychiatry Res*, Vol. 156, pp. 1–13, Oct 2007.

12. Okada, F., Y. Tokumitsu, Y. Hoshi, and M. Tamura, "Impaired interhemispheric integration in brain oxygenation and hemodynamics in schizophrenia.," *Eur Arch Psychiatry Clin Neurosci*, Vol. 244, no. 1, pp. 17–25, 1994.

13. Fallgatter, A. J., and W. K. Strik, "Reduced frontal functional asymmetry in schizophrenia during a cued continuous performance test assessed with near-infrared spectroscopy.," *Schizophr Bull*, Vol. 26, no. 4, pp. 913–919, 2000.

14. Kubota, Y., M. Toichi, M. Shimizu, R. A. Mason, C. M. Coconcea, R. L. Findling, K. Yamamoto, and J. R. Calabrese, "Prefrontal activation during verbal fluency tests in schizophrenia–a near-infrared spectroscopy (nirs) study.," *Schizophr Res*, Vol. 77, pp. 65–73, Sep 2005.

15. Suto, T., M. Fukuda, M. Ito, T. Uehara, and M. Mikuni, "Multichannel near-infrared spectroscopy in depression and schizophrenia: cognitive brain activation study.," *Biol Psychiatry*, Vol. 55, pp. 501–511, Mar 2004.

16. Andreasen, N. C., S. Paradiso, and D. S. O'Leary, ""cognitive dysmetria" as an integrative theory of schizophrenia: a dysfunction in cortical-subcortical-cerebellar circuitry?," *Schizophr Bull*, Vol. 24, no. 2, pp. 203–218, 1998.

17. Weinberger, D. R., M. F. Egan, A. Bertolino, J. H. Callicott, V. S. Mattay, B. K. Lipska, K. F. Berman, and T. E. Goldberg, "Prefrontal neurons and the genetics of schizophrenia.," *Biol Psychiatry*, Vol. 50, pp. 825–844, Dec 2001.

18. Watanabe, A., and T. Kato, "Cerebrovascular response to cognitive tasks in patients with schizophrenia measured by near-infrared spectroscopy.," *Schizophr Bull*, Vol. 30, no. 2, pp. 435–444, 2004.

19. Barch, D. M., C. S. Carter, and J. D. Cohen, "Factors influencing stroop performance in schizophrenia.," *Neuropsychology*, Vol. 18, pp. 477–484, Jul 2004.

20. Boucart, M., N. Mobarek, C. Cuervo, and J. M. Danion, "What is the nature of increased stroop interference in schizophrenia?," *Acta Psychol (Amst)*, Vol. 101, pp. 3–25, Mar 1999.

21. Emir, U. E., "System characterization for a fast optical imager," Master's thesis, Boğaziçi University, 2001.

22. Gratton, G., J. S. Maier, M. Fabiani, W. W. Mantulin, and E. Gratton, "Feasibility of intracranial near-infrared optical scanning.," *Psychophysiology*, Vol. 31, pp. 211–215, Mar 1994.

23. Perlstein, W. M., C. S. Carter, D. C. Noll, and J. D. Cohen, "Relation of prefrontal cortex dysfunction to working memory and symptoms in schizophrenia.," *Am J Psychiatry*, Vol. 158, pp. 1105–1113, Jul 2001.

24. Schroeter, M. L., S. Zysset, T. Kupka, F. Kruggel, and D. Y. von Cramon, "Near-infrared spectroscopy can detect brain activity during a color-word matching stroop task in an event-related design.," *Hum Brain Mapp*, Vol. 17, pp. 61–71, Sep 2002.

25. Schroeter, M. L., S. Zysset, M. Wahl, and D. Y. von Cramon, "Prefrontal activation due to stroop interference increases during development–an event-related fnirs study.," *Neuroimage*, Vol. 23, pp. 1317–1325, Dec 2004.

26. Takizawa, R., K. Kasai, Y. Kawakubo, K. Marumo, S. Kawasaki, H. Yamasue, and M. Fukuda, "Reduced frontopolar activation during verbal fluency task in schizophrenia: A multi-channel near-infrared spectroscopy study.," *Schizophr Res*, Dec 2007.

27. Zysset, S., K. Müller, G. Lohmann, and D. Y. von Cramon, "Color-word matching stroop task: separating interference and response conflict.," *Neuroimage*, Vol. 13, pp. 29–36, Jan 2001.